Pergamon

PII: S0967-0645(96)00041-0

Deep-Sea Research II, Vol. 43, No. 7–8, pp. 1439–1471, 1996
Published by Elsevier Science Ltd
Printed in Great Britain.
0967-0645/96 $15.00 + 0.00

Historical and recent evidence of Scotian Shelf Water on southern Georges Bank

J. J. BISAGNI,* R. C. BEARDSLEY,† C. M. RUHSAM,*‡ J. P. MANNING§ and W. J. WILLIAMS†

(*Received* 29 *September* 1994; *in revised form* 29 *November* 1995; *accepted* 6 *May* 1996)

Abstract—Historical data from 1912–1987 indicate that low salinity (less than 32.0 psu) near-surface water occurs occasionally on southern Georges Bank during May, while none occurs during April. Composite monthly plots of historical near-surface salinity and estimated advection rates show that the southwestern Scotian Shelf is the immediate upstream source of this low salinity water. Optimally interpolated satellite-derived SST and hydrographic data reveal that very cold (less than 2.0°C), low salinity (less than 32.0 psu) Scotian Shelf Water (SSW), initially located south of the 200-m isobath off southern Georges Bank in early March 1992, moved north onto southern Georges Bank during April 1992. SSW was not as extensive during the same period in 1993, as evidenced by significantly higher temperatures and salinities. These differences show large interannual variability in the transport and/or properties of SSW flowing onto Georges Bank. Lower (higher) salinities measured during spring 1992 (1993) on southern Georges Bank are consistent with higher (lower) St Lawrence River discharge noted during spring 1991 (1992) and the ~nine month lag between annual discharge maxima from rivers located upstream and minimum salinity at Cape Sable in February. However, comparisons between historical occurrences of low salinity (less than 32.0 psu) SSW on southern Georges Bank noted for May 1966, 1971 and 1978, and cumulative St Lawrence River discharge from the spring prior to each occurrence, show no relationship. This suggests that the occurrence of low salinity water on southern Georges Bank is not directly related to variations in upstream river discharge.

Although an idealized model of wind forcing on a bank-trapped density front shows that near-surface flow is related to superposition of an Ekman layer and the along-bank gyral circulation, evidence from late winter–spring 1992 and 1993 on Georges Bank shows that except for on-bank movement of the shelf-slope front during late spring 1992, simple Ekman theory does not explain on-bank movement of the SSW plume during 1992 nor the immobile nature of the shelf-slope front during late winter 1992 and late winter–spring 1993. Surface heat flux and satellite-derived SST from Georges Bank and the Scotian Shelf together with a slab mixed-layer model allows estimation of the advective heat flux and transport of SSW flowing onto Georges Bank from the Scotian Shelf during late winter–spring 1992. Mean advective heat flux onto Georges Bank during March–May 1992 is $-14.5\ \mathrm{mW\ cm^{-2}}$ with an estimated error of $\sim 3.5\ \mathrm{mW\ cm^{-2}}$, demonstrating that advection of cold SSW onto Georges Bank is required. Mean velocity and transport of SSW flowing onto Georges Bank during March–May 1992 are $13.4\ \mathrm{cm\ s^{-1}}$ and 0.21 Sv, assuming a SSW depth (width) of 40 m (40 km), demonstrating that flow of SSW onto Georges Bank was robust during the period. At this time, the dynamics that control the flow of SSW across Northeast Channel are unknown. Published by Elsevier Science Ltd

*NOAA/National Marine Fisheries Service, Northeast Fisheries Science Center, 28 Tarzwell Drive, Narragansett, RI 02882, U.S.A.

†Woods Hole Oceanographic Institution, Woods Hole, MA 02543, U.S.A.

‡Present address: NOAA/National Environmental Satellite Data and Information Service, Woods Hole, MA 02543, U.S.A.

§NOAA/National Marine Fisheries Service, Northeast Fisheries Science Center, Water Street, Woods Hole, MA 02543, U.S.A.

INTRODUCTION

Georges Bank is a large submarine bank located southeast of Cape Cod, partially separating the Gulf of Maine (GOM) from the North Atlantic (Fig. 1). The primary connections between the GOM and the North Atlantic are Northeast Channel and Great South Channel located east and west of Georges Bank, respectively. Browns Bank and the Scotian Shelf lie east of Northeast Channel, while Nantucket Shoals and the Mid-Atlantic Bight lie west of Great South Channel.

Oceanographers have long known about the flow of cold, low salinity Scotian Shelf Water (SSW), which enters the GOM south of Cape Sable (Bigelow, 1927; Redfield, 1939). A thermohaline box model of the GOM requires near-surface input of SSW, which is mixed to mid-depth during winter with warm, high salinity slope water entering at depth through Northeast Channel (Brown and Beardsley, 1978). The product of this deep mixing is Maine intermediate water, which exits and flows into the Mid-Atlantic Bight (Brown and Beardsley, 1978). Hydrographic data compiled by Colton *et al.* (1968) suggest that SSW inputs to the GOM between the surface and intermediate depths are a regular winter occurrence (Hopkins and Garfield, 1979).

Direct long-term measurements of currents and water properties along a transect from Cape Sable and across Browns Bank show a seasonal maximum in the flow of SSW into the GOM, together with a salinity minimum during early February (Smith, 1983, 1989a, 1989b). An upstream source for the February salinity minimum is peak discharge from the St Lawrence, Ottawa and Saguenay Rivers (RIVSUM) about 9 months prior to maximum inflow (Sutcliffe *et al.*, 1976; Koslow *et al.*, 1986; Smith, 1989b). However, oxygen isotope data show continuity of SSW extending to higher latitudes than the Gulf of St Lawrence (Fairbanks, 1982; Chapman *et al.*, 1986), to as far north as the Labrador Sea and the southern coast of Greenland by way of the southward-flowing coastal current (Chapman and Beardsley, 1989).

The flow of SSW across Northeast Channel and onto Georges Bank from the southwestern Scotian Shelf during winter has not been studied as extensively as the Cape Sable winter inflow. Early data suggest cross-channel flow, as evidenced by westward progress of the 32.5 psu isohaline across Northeast Channel to within several kilometers of Georges Bank between February and April 1920 (Bigelow, 1927). Historical data support cross-channel SSW flow onto Georges Bank and the existence of SSW along the Bank's southern flank but do not support winter intrusion of SSW onto central Georges Bank (Hopkins and Garfield, 1981). Recent data show SSW on southern Georges Bank during February 1978 and March 1979, reaching depths of 40 m and 60 m, respectively (EG&G, 1980; Flagg, 1987). In addition, an analysis of the seasonal cycle of shelf water volume on Georges Bank shows an early winter maximum (Mountain, 1991) occurring at nearly the same time as the Cape Sable salinity minimum (Smith, 1983, 1989a, 1989b) possibly suggesting winter occurrence of SSW on Georges Bank.

Motivation for this work is to formulate a better understanding of interannual variability of near-surface waters on southern Georges Bank that is related to flow of SSW across Northeast Channel during late winter–spring. This interannual variability may play an important role in the spatial and temporal distribution of density stratification and recruitment of zooplankton and ichthyoplankton on Georges Bank. We believe the interannual variability noted on southern Georges Bank between late winter–spring 1992 and 1993, from data collected by satellites, ships and moored platforms, is related to

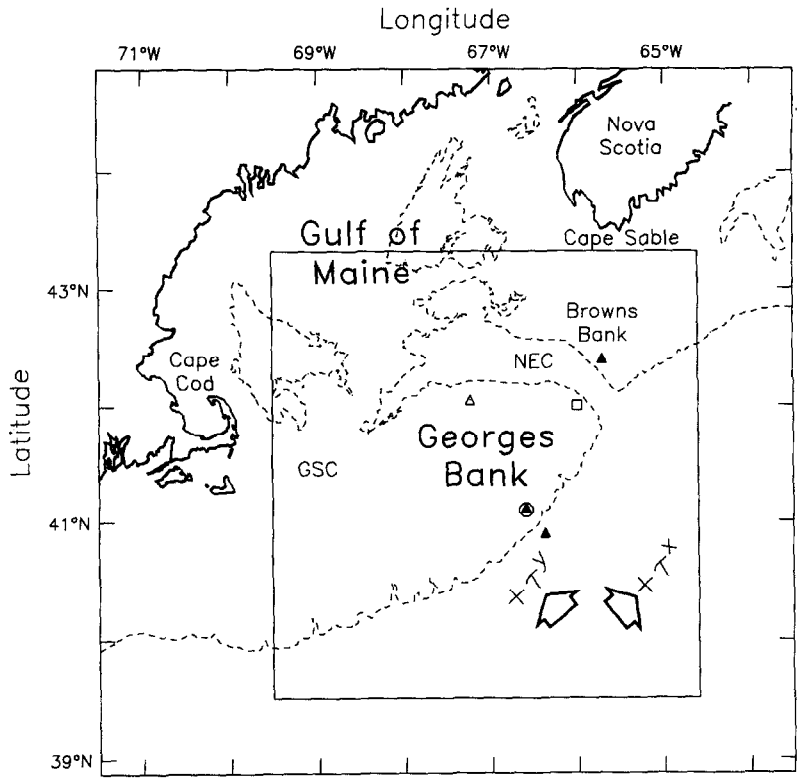

Fig. 1. Georges Bank study area together with the locations of the OI SST mapping region (box), Northeast Channel (NEC), Great South Channel (GSC), 200-m isobath (dashed), NOAA data buoy 44011 (circle), FNOC wind grid point (square), four OI SST time-series (triangles) and three surface heat flux estimation points (solid triangles). Also shown are the positive along-bank (τ^x) and cross-bank (τ^y) wind stress directions (arrows).

differences in the transport and/or properties of SSW crossing Northeast Channel and factors controlling the position of the shelf break front on southern Georges Bank.

The objectives of this analysis are:

1. to investigate the historical occurrence of low salinity SSW flowing across Northeast Channel and onto southern Georges Bank,
2. to describe the interannual variability of southern Georges Bank near-surface waters between late winter–spring 1992 and 1993 and its relationship to variations in upstream river discharge and local wind stress, and
3. to estimate the advective heat flux and transport of cold SSW flowing onto Georges Bank from the southwestern Scotian Shelf during late winter–spring 1992 using surface heat flux estimates and inverse techniques.

DATA AND METHODS

Historical hydrographic data

Historical hydrographic data from the Scotian Shelf, Georges Bank, and Gulf of Maine

regions were obtained from a NODC data base (NODC, 1991) for the period 1912–1987. Data were first sorted by month and then used to determine the geographic limits of near-surface low salinity water during late spring. After inspection of the hydrographic data obtained from southern Georges Bank during spring 1992 (described below) and the historical hydrographic data, a salinity of 32.0 psu was chosen as an upper limit to identify the freshest water that can occur over the southeastern Scotian Shelf in late winter.

Satellite-derived sea surface temperatures

Advanced Very High Resolution Radiometer (AVHRR) data collected from 27 February to 1 June 1992 (1 March–8 June 1993) by the NOAA-11 polar-orbiting satellite were preprocessed (Cornillon *et al.*, 1987), resulting in 96 (71) 1-km resolution, morning and evening sea surface temperature (SST) images that spanned the 1992 (1993) late winter–spring period. Cold SST biases caused by clouds were eliminated by automated (Cayula and Cornillon, 1992) and manual (Bisagni and Sano, 1993) flagging procedures.

SST values were extracted from each cloud-flagged image using an ~11-km resolution grid over a mapping region spanning Georges Bank and the southwestern Scotian Shelf (Fig. 1). A mean SST was determined for each grid point by averaging all non-cloud pixels within a 11×11 pixel array. If the percentage of cloud-flagged pixels in an array reached 50% or more, a mean SST was not computed. The seasonal SST signal was removed from the time-series at each grid point using harmonic regression and significance tests (Brownlee, 1965; Fofonoff and Bryden, 1975).

Five-day averaged SST residuals were produced at five-day intervals beginning (ending) at noon on yearday 61 (156) of 1992 and 1993 from the temporally "gappy" SST data at each grid point using optimal interpolation (OI) (Chelton and Schlax, 1991). OI also allows computation of the error as a fraction of the non-seasonal SST root-mean-square (rms) variability for each estimate. Weights used in the interpolation were computed using an analytical function fitted to the raw autocorrelation computed from 1985–1987 daily averaged near-surface (~1-m depth) temperatures from NOAA buoy 44011 located on Georges Bank (Fig. 1). Maximum time lag between an OI estimate and input observations was initially set to 5 days. The number of observations used to compute each OI estimate was set to 8. Mean non-seasonal SST signal variance was calculated to be 0.91 $(°C)^2$ while the SST noise variance at any grid point was estimated to be 0.06 $(°C)^2$, given an rms uncertainty of 0.75°C for a single SST retrieval and 10 degrees of freedom.

Restoration of the seasonal SST signal to the residuals resulted in 20, five-day averaged OI SST and error maps for 1992 and 1993. Four OI SST maps from each year, (yeardays 60.5, 90.5, 120.5 and 155.5) are shown (Plates 1 and 2). Comparison of "same day" input SST observations with output OI SST estimates having errors of less than 0.5 from a 1982 Gulf of Maine analysis, display a rms difference of 0.72°C ($N = 39\,322$) and a correlation coefficient of 0.98 ($p \leq 0.05$) (Bisagni *et al.*, 1996). Comparison of five-day averaged near-surface temperatures from NOAA buoy 44011 with five-day averaged OI SST values for 1992 from this study yields a rms difference of 0.47°C ($N = 16$) and a correlation coefficient of 0.95 ($p \leq 0.05$).

Mean SST and error time-series were computed from the 20 OI maps for each year at 10 grid points oriented parallel to the local bathymetry at four locations: ONGBS (inshore of the 200-m isobath along southern Georges Bank), OFFGBS (offshore of the 200-m isobath along southern Georges Bank), ONGBN (inshore of the 200-m isobath along northern

Georges Bank), and ONSS (inshore of the 200-m isobath along the southwestern Scotian Shelf) (Fig. 1, Plates 1 and 2). SST time-series also were extracted along a cross-bank transect from the 20 OI maps from each year (Plates 1 and 2).

Shipboard and moored hydrographic data

Oblique water column profiles of temperature and salinity were measured using a CTD profiler during 38 (33) bongo net hauls conducted from *Albatross IV* cruise AL9204, 27 April–8 May 1992, (AL9205, 18–29 May 1992) on southern Georges Bank (Manning *et al.*, 1995). Hydrographic data were also collected along a transect across southern Georges Bank during R.V. *Endeavor* cruise EN237, 19–28 May 1992, using a CTD profiler and a CTD mounted on a towed video plankton recorder (Davis *et al.*, 1992). An additional hydrographic survey of southern Georges Bank was completed using a CTD profiler during 47 bongo net hauls conducted from *Albatross IV* (AL9306, 18–28 May 1993). Temperature and salinity errors are approximately ± 0.01°C and ± 0.02 psu (M. Taylor, personal communication, 1994).

Survey stations from AL9204 are the most widespread (Figs 2 and 3). Stations from AL9205 and AL9306, while less widespread, have about the same spatial coverage (Figs 2 and 3) but are separated by 1 year. The EN237 transect spanned depths from less than 50 m on central Georges Bank to greater than 300 m over the continental slope (Fig. 2).

A decade-long (May 1984–March 1994) time-series of near-surface ($\sim$1-m depth) temperature from NOAA data buoy 44011 located on southern Georges Bank (Fig. 1) was used to calculate long-term, monthly-mean temperatures. Hourly data were preprocessed using a 10-h running average. All values greater than 2 standard deviations within the 10-h period were removed. A long-term monthly-mean temperature and standard deviation were computed for each month from only those months possessing at least 2 weeks of data. Based on this criterion, 82% of the months were included in the analysis. Monthly-mean temperatures were computed for January–October 1992, thus covering the late winter–spring 1992 period. Data were not available from buoy 44011 for November–December 1992 and again for January–April 1993, precluding a similar analysis for late winter–spring 1993.

Wind stress

Six-hourly Fleet Numerical Oceanography Center (FNOC) model wind velocity was obtained at 42°N, 66°W on Georges Bank (Fig. 1). Wind velocity was adjusted to the sea surface by rotating the wind vector 15° anti-clockwise and reducing its magnitude by 30% (Bakun, 1975). Good agreement has been demonstrated between measured wind velocity and adjusted FNOC model values for periods as short as 2 days off the British Columbia coast (Thomson, 1983) and on the Grand Banks (DeYoung and Tang, 1989).

Six-hourly adjusted wind velocity was converted to wind stress using bulk formulae (Large and Pond, 1981) and was used to compute monthly-averaged wind stress for 24 consecutive months (July 1991–June 1993). Long-term mean monthly-averaged wind stress also was computed from a 26 year (1967–1992) record of six-hourly estimates. In addition, five-day averaged wind stress was computed from six-hourly estimates for the 1992 and 1993 SST analysis time periods described above. Monthly and five-day averaged stresses were

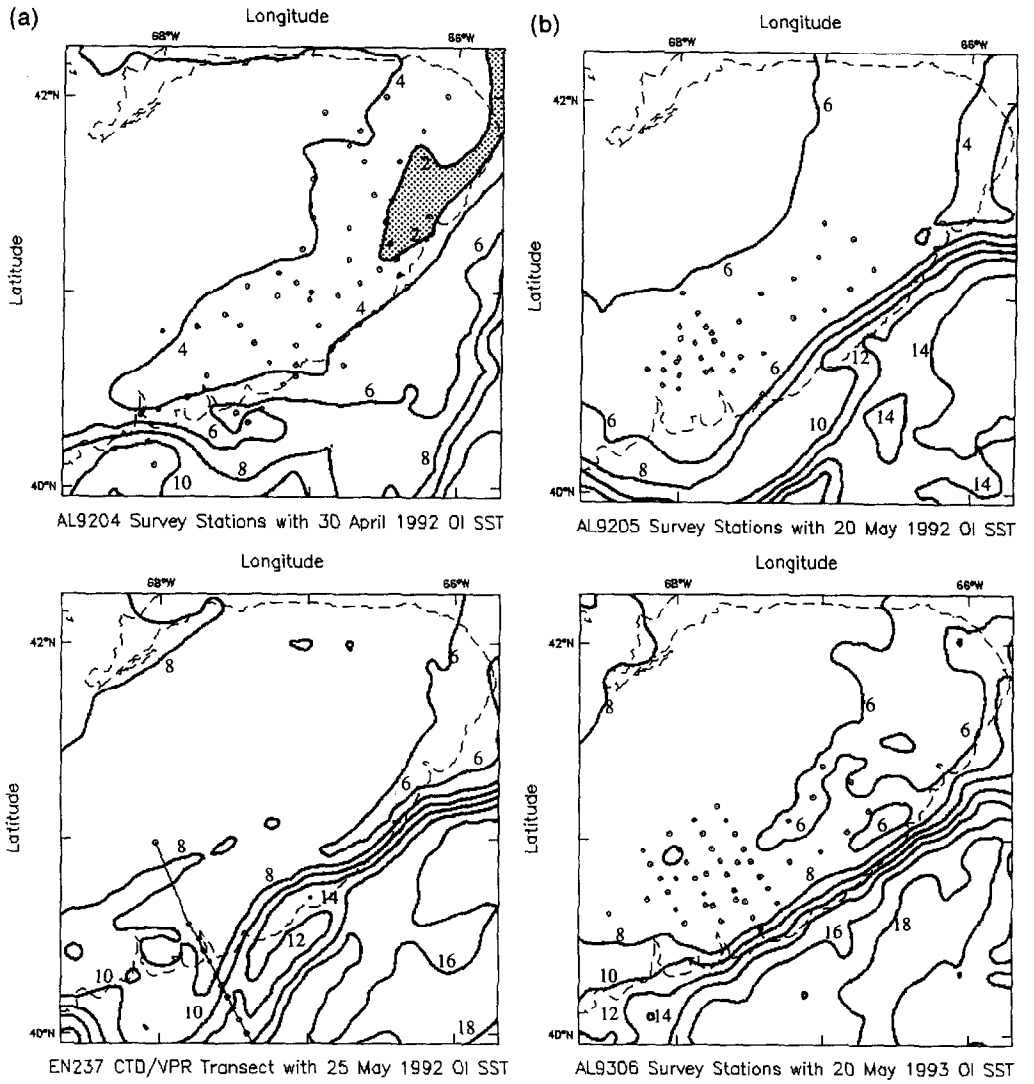

Fig. 2. CTD station locations conducted on Georges Bank during *Albatross IV* cruises AL9204, AL9205 and AL9306 and the location of the 26–27 May 1992 CTD transect from R.V. *Endeavor* cruise EN237. Also shown is SST (contour interval = 2°C) from the OI SST map closest to the mid-point of each cruise period and the 200-m isobath (dashed). SST ≤2.0°C is shaded.

transformed into along-bank (τ^x) and cross-bank (τ^y) stress components (Fig. 1) by rotating the coordinate system 43.2° anti-clockwise, resulting in $+\tau^x$ ($+\tau^y$) being oriented parallel (perpendicular) to the local bathymetry near 41.1°N, 66.6°W towards 43.2°T (313.2°T).

St Lawrence river discharge

Monthly-averaged discharge was obtained for 1991–1992 from the La Salle gauging station (020A016) located on the St Lawrence River. Monthly-averaged discharge values

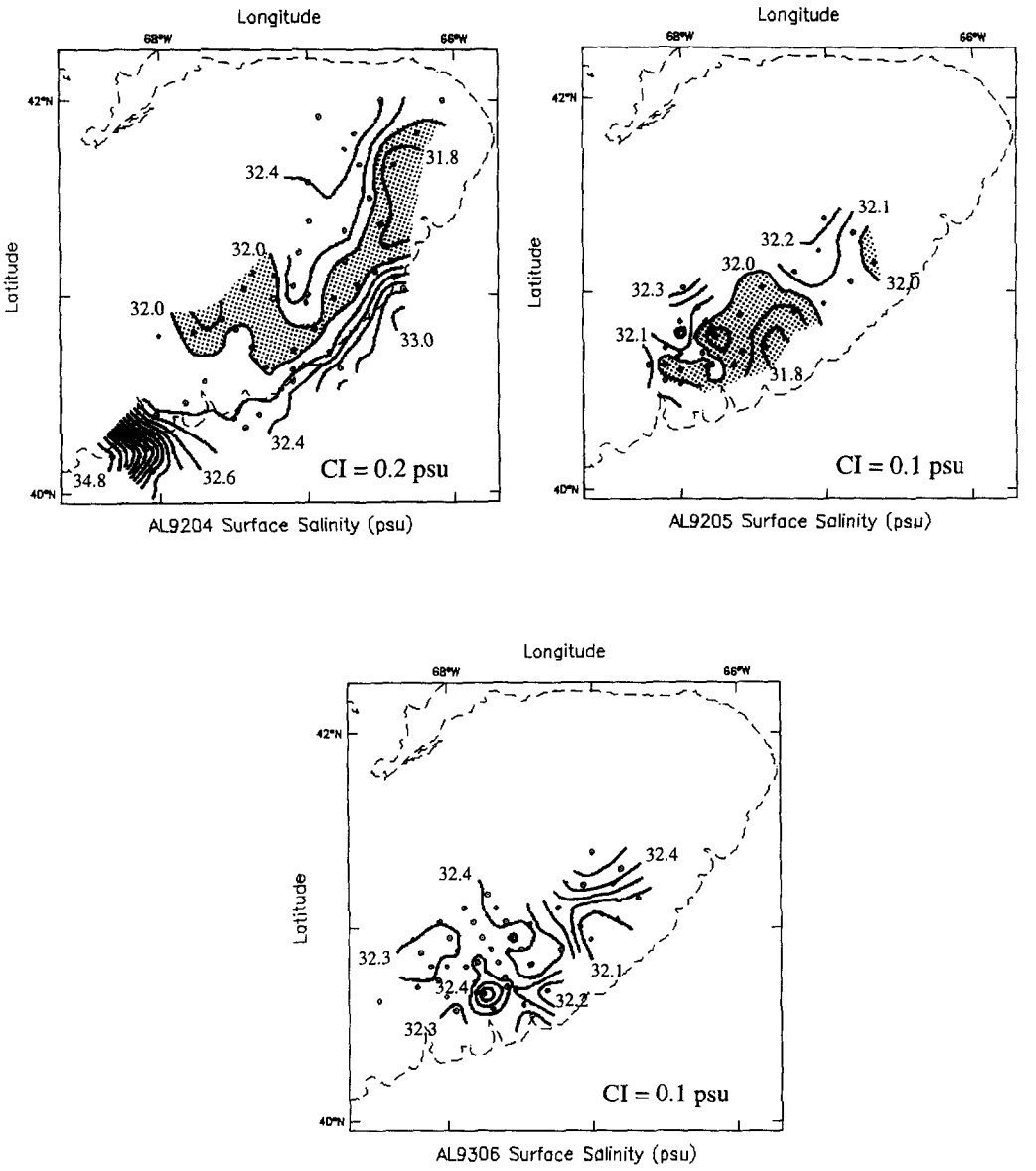

Fig. 3. CTD station locations conducted on Georges Bank during *Albatross IV* cruises AL9204, AL9205 and AL9306. Also shown are near-surface salinity contours from each cruise. Contour intervals (CI) are indicated. Salinity $\leq$32.0 psu is shaded.

from 1991 and 1992 were compared with the 38 year (1955–1992) long-term mean monthly-averaged discharge and standard deviation values. Monthly cumulative volumes were computed for 1991 and 1992 from the monthly-averaged discharge values, while the per cent change by month between corresponding months of 1991 and 1992 (relative to the 1992 monthly cumulative volumes) was also computed.

Table 1. *Means and standard deviations of the five-day-averaged bulk aerodynamic and radiational heat flux components* (mW cm^{-2}) *at three time series locations, spring 1992*

Location	Q_{sw}	Q_{lw}	Q_e	Q_s	Q_{net}
OFFGBS	20.0±5.7	3.6±1.4	3.5±2.4	2.0±2.5	10.9±4.7
ONGBS	20.0±5.7	3.4±1.3	1.2±1.5	−0.2±1.6	15.7±6.8
ONSS	20.0±5.7	3.4±1.3	0.3±1.2	−1.2±1.0	17.6±6.3

Surface heat flux

Surface heat flux was estimated for yeardays 77–156* (17 March–4 June) 1992 at three locations (Fig. 1): ONGBS (coincident with NOAA data buoy 44011); OFFGBS (~30 km southeast of buoy 44011); and ONSS (~150 km northeast of buoy 44011). Daily-averaged net incident shortwave radiational heat flux (Q_{sw}) is assumed to be identical at each location and equal to the value computed from total daily shortwave radiation measured atop the Clark Laboratory in Woods Hole, MA, after correction for mean albedo (Payne, 1972). We will assume that the total error of daily-averaged Q_{sw} at each offshore location is equal to the 3% sensor error in the total daily radiation measurements at Woods Hole (R. Payne, personal communication, 1994). Q_{sw} biases at each offshore location, relative to the measurements at Woods Hole, cannot be determined due to a lack of Q_{sw} measurements on Georges Bank during the 1992 study period. Therefore, Q_{sw} biases at each of the offshore locations are assumed to be zero.

Daily averages of sensible (Q_s) and latent (Q_e) heat losses were estimated using bulk formulae (Friehe and Schmitt, 1976), interpolated daily-averaged OI SST, air temperatures and wind speed from NOAA data buoy 44011 along with monthly-averaged humidity values from long-term (1941–1972) air and dew point temperatures (Joyce, 1987). Errors associated with Q_s and Q_e determined from bulk estimates may be as high as 0.8 and 1.5 mW cm^{-2}, respectively, based on comparisons with direct flux measurements (Friehe and Schmitt, 1976).

Daily averages of net longwave radiational heat losses (Q_{lw}) were estimated using Efimova's formula (Budyko, 1974) as discussed by Simpson and Paulson (1979) after correction for a cloud factor (Reed, 1976, 1977). The error associated with use of this method for estimates of daily-averaged Q_{lw} is 2 mW cm^{-2} (Simpson and Paulson, 1979).

Five-day averaged net surface heat flux (Q_{net}) was computed at ONGBS, OFFGBS and ONSS using

$$Q_{net} = Q_{sw} - Q_{lw} - Q_e - Q_s \tag{1}$$

to coincide with five-day averaged OI SST time-series and Georges Bank wind stress time-series. Using a constant value of 0.6 mW cm^{-2} to represent the 3% error in mean Q_{sw} at each location (Table 1), the total error for daily-averaged Q_{net} is the sum of individual errors or ~4.9 mW cm^{-2}. Total error for five-day averaged Q_{net} was estimated to be ~3.5 mW cm^{-2} by decreasing the error for daily-averaged Q_{net} by a factor of $1/\sqrt{2}$ to account for $N=2$ independent samples during the 5-day averaging period, as suggested by meteorological variability within the ~5-day-period "weather band". This value agrees with the approximate error estimated for Q_{net} at Emerald Basin located on the Scotian Shelf (Umoh and Thompson, 1994).

*A data outage for NOAA buoy 44011 prevented estimates of bulk heat fluxes for yeardays 61–76.

RESULTS

Historical hydrographic conditions

The historical hydrographic data can be used to infer the movement of less saline SSW onto Georges Bank during late winter–spring, provided there is adequate sampling. The locations of all historical hydrographic stations and the subset with near-surface salinity less than 32.0 psu are shown for the months of April and May (Fig. 4). In April, water with a salinity of less than 32.0 psu is found over the Scotian Shelf, extreme northeastern Georges Bank, off the mouth of the Bay of Fundy and in the nearshore area of the western Gulf of Maine, the latter due to local runoff. Note that no water with salinity less than 32.0 psu has been found over southern Georges Bank in April despite adequate sampling during April 1940, 1941, 1966, 1974, 1981 and 1985. In May, water with less than 32.0 psu is found over both the southern flank and northwestern flanks of Georges Bank, with higher salinity water covering the top of the bank separating these two lower salinity waters.

This April–May sequence of near-surface low salinity water suggests two possible upstream sources of the freshest waters found over the southern flank of Georges Bank in May: the Scotian Shelf and the western Gulf of Maine. An estimate of the time required for low salinity water to be advected from the western Gulf of Maine source region around the northern flank of Georges Bank to the southern flank area by May can be made from the trajectories of satellite-tracked drifters deployed in spring in the western Gulf of Maine and drogued at 2 m and 10 m (W. R. Geyer, personal communication, 1994) and 5 m and 50 m (Limeburner and Beardsley, 1982): the minimum advective time is 40–50 days, which is too long to explain the observed pattern (Fig. 4). In addition, maps of surface salinity in the Great South Channel region show the 32.0 psu contour to be west of Cape Cod in late April, as far east as the Great South Channel in mid-May, and near the eastern end of Georges Bank in early June (Chen, 1992; Limeburner and Beardsley, 1989). From these positions, water with salinity less than 32.0 psu could not be advected to the southern flank of Georges Bank during May.

We conclude that the Scotian Shelf must be the source of the freshest waters (salinity less than 32.0 psu) found over the southern flank of Georges Bank during May. Water with salinity of less than 32.0 psu has been found on southern Georges Bank during May of 1941, 1954, 1966, 1971, and 1978 in the NODC historical data base examined here. Furthermore, Georges Bank was sampled adequately in May of 1934, 1940, 1941, 1965, 1966, 1978, 1979, 1982, 1984 and 1985, i.e. 10 of the 76 years within the historical data period examined. Thus, waters with salinity less than 32.0 psu were found on southern Georges Bank during May in three out of the 10 years (1941, 1966 and 1978) when Georges Bank was well sampled.

Interannual sea surface temperature variability

OI SST values from southern Georges Bank display significant variability between spring 1992 and 1993 (Plates 1–3). The SST map for yearday 60.5, 1992 shows a large mass of very cold ($\sim$2°C) water extending southwestward from the Scotian Shelf across Northeast Channel and along southern Georges Bank (Plate 1). A similar mass of water, possessing an SST of $\sim$2°C, was largely absent during 1993, when very cold water extended only onto northeastern-most Georges Bank by yearday 60.5 (Plate 2). Volume renderings of OI SST map time-series from 1992 and 1993 clearly show the interannual SST variability (Plate 3).

On-bank movement of cold SSW is indicated between yeardays 60.5 and 120.5 1992, until by yearday 120.5, the loci of SST minima associated with the SSW plume lay bankward of the 200-m isobath and parallel to local bathymetry (Plate 1). Minimum SST values within the SSW plume warmed to ~6–7°C by yearday 155.5 at the end of each time-series. Warm-core Gulf Stream rings, present during both years, were initially located farther offshore during 1992 than 1993 when the northern margins of two rings lay just offshore of the 200-m isobath (Plates 1 and 2).

OI SST time series at ONGBS, OFFGBS, ONSS and ONGBN also show spatial and interannual differences (Fig. 5). SST was coldest at ONSS, while SST at ONGBN was virtually always warmer than at ONGBS. The largest interannual SST variability occurred at OFFGBS during March–April. Spring 1992 showed OFFGBS SST approaching minimum values at ONSS during early March, increasing slowly ($\sim 0.05°C\,day^{-1}$) through late April, surpassing values at ONGBS and ONGBN by early and mid-April, respectively, followed by a much more rapid ($\sim 0.3°C\,day^{-1}$) increase during May and June. However, spring 1993 showed that SST at OFFGBS remained ~6–12°C higher than at other locations during the period, increasing by an average of $\sim 0.05°C\,day^{-1}$. OI error time-series show higher errors in 1993 than 1992, due to the larger number of cloud-covered images during spring 1993 (Fig. 5).

Interannual hydrographic variability

Near-surface data from AL9204 (AL9205) during late April–early May (late May) 1992 reveal temperatures as low as ~2°C (~4°C) and salinities less than 32.0 psu near the axis of the SSW plume for both cruises (Figs 2 and 3). Near-surface data from AL9204 and AL9205 demonstrate a positive temperature–salinity correlation, while mean near-surface salinity for AL9205 is not significantly different from AL9204 (Fig. 6). However, mean near-surface temperature from AL9205 (late May 1992) is ~2°C higher than during AL9204 (Fig. 6), consistent with seasonal warming of surface waters described for southern Georges Bank (Bisagni, 1992). Sub-surface data from the EN237 (late May 1992) transect show a narrow jet of cold (less than 4°C), low salinity (less than 32.5 psu) water at a distance of ~80 km along the transect, extending to depths of ~50 m, corresponding to the SSW plume (Fig. 7).

Hydrographic data from AL9306 (late May 1993) show near-surface waters were warmer and more saline than during AL9205, 1 year earlier (Figs 2 and 3). As in 1992, near-surface data from 1993 demonstrate a positive temperature–salinity correlation. Near-surface mean temperature (mean salinity) was ~1.8°C warmer (~0.4 psu more saline) than during AL9205, 1 year earlier (Fig. 6). Thus, the extensive, exceptionally cold and low salinity water noted on southern Georges Bank during spring 1992 was nearly absent during spring 1993.

Monthly-averaged, near-surface temperatures from NOAA buoy 44011 on southern Georges Bank during spring 1992 were greater than 1 standard deviation lower (up to ~3°C colder) than the long-term monthly mean (Fig. 8). Temperature statistics from other locations on southern Georges Bank may differ due to the nature of the single-point measurement at buoy 44011. However, despite this uncertainty, near-surface temperature data from buoy 44011 together with the shipboard and satellite-derived SST evidence (described above) strongly suggest the widespread occurrence of anomalously-cold water on southern Georges Bank during late winter–spring 1992.

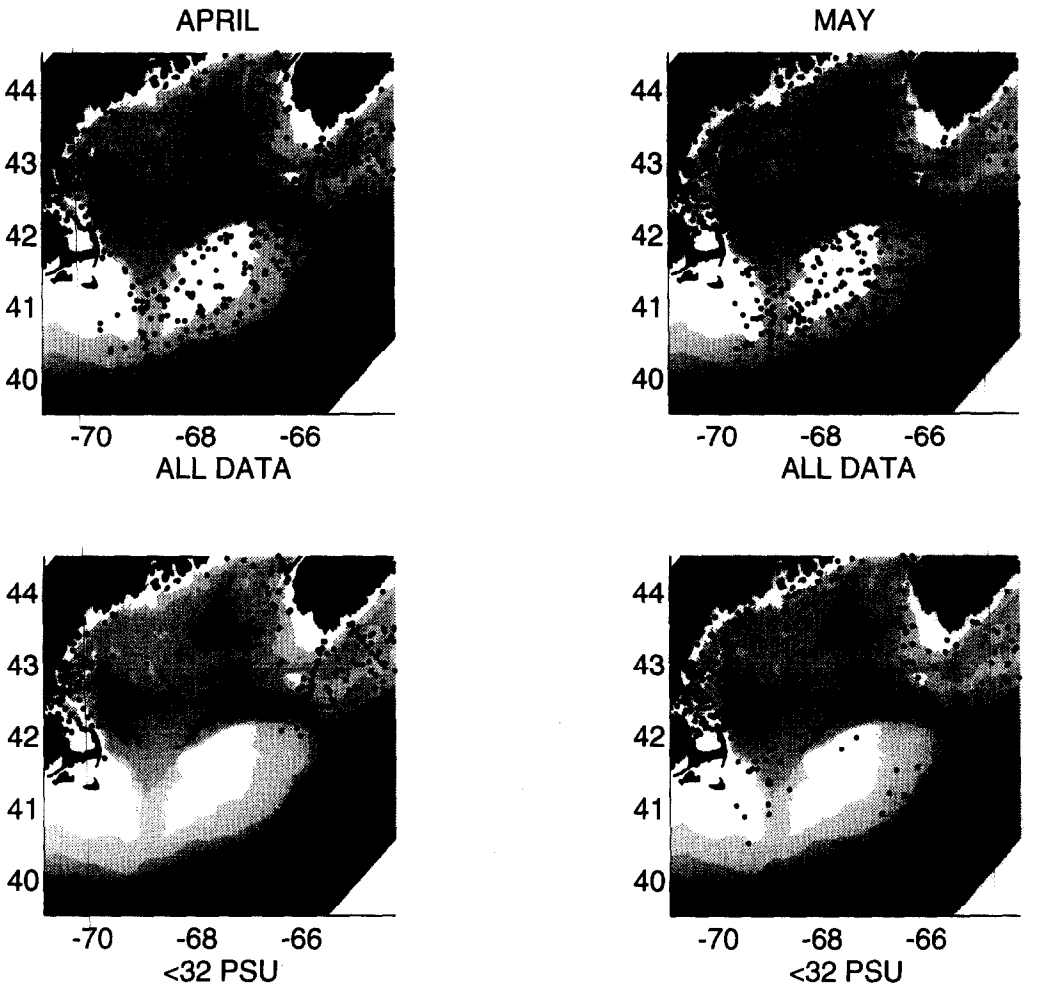

Fig. 4. The positions of all hydrographic stations made in the months of April and May in the NODC historical data base (upper panels), and the positions of the subset of stations for each month with near-surface salinities less than 32.0 psu.

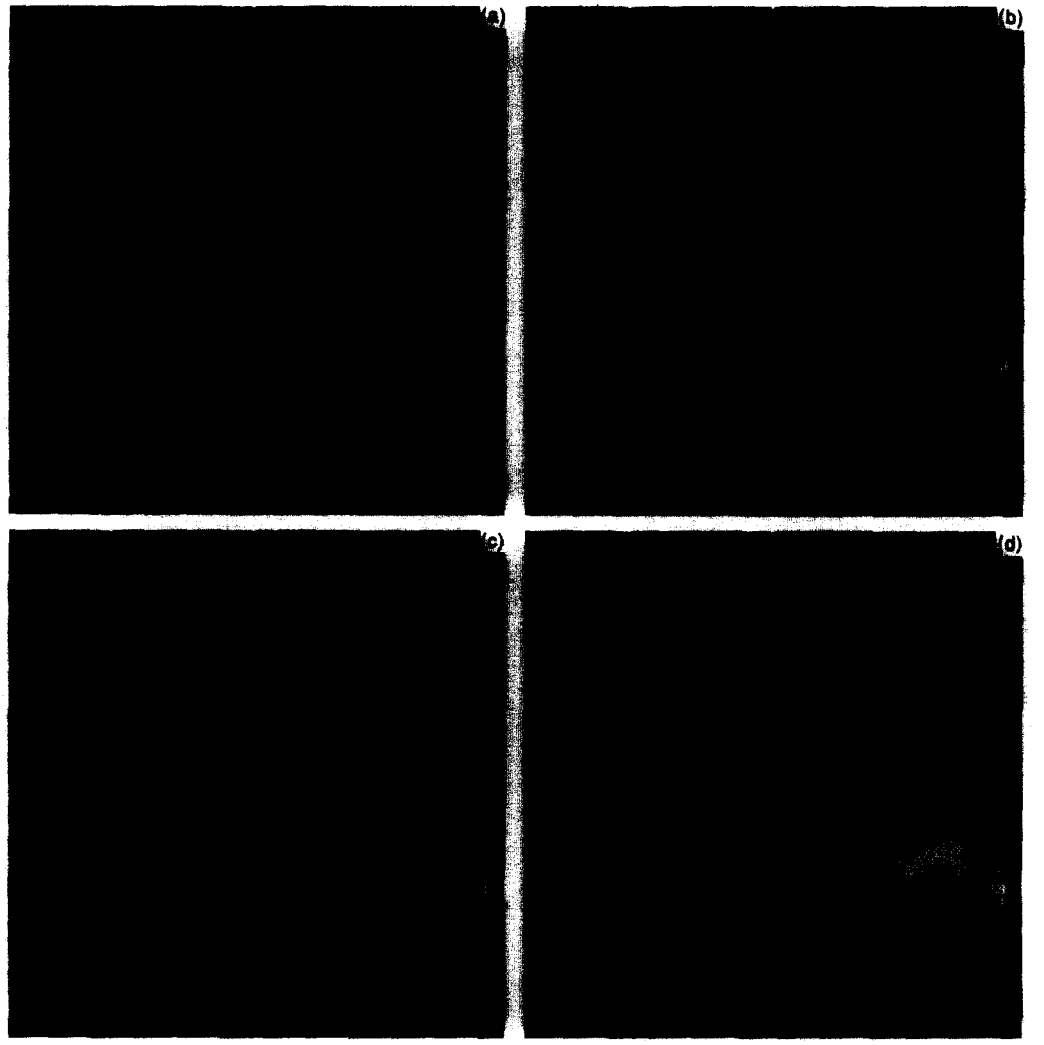

Plate 1. Five-day averaged OI SST maps for 1 March, 31 March, 30 April and 4 June 1992 for the mapping region shown in Fig. 1 along with a SST color table (°C). Also shown are the locations of four sets of grid points used for extraction of mean OI SST time-series shown in Fig. 5 (crosses) and the cross-bank transect used for extraction of OI SST values shown in Fig. 13.

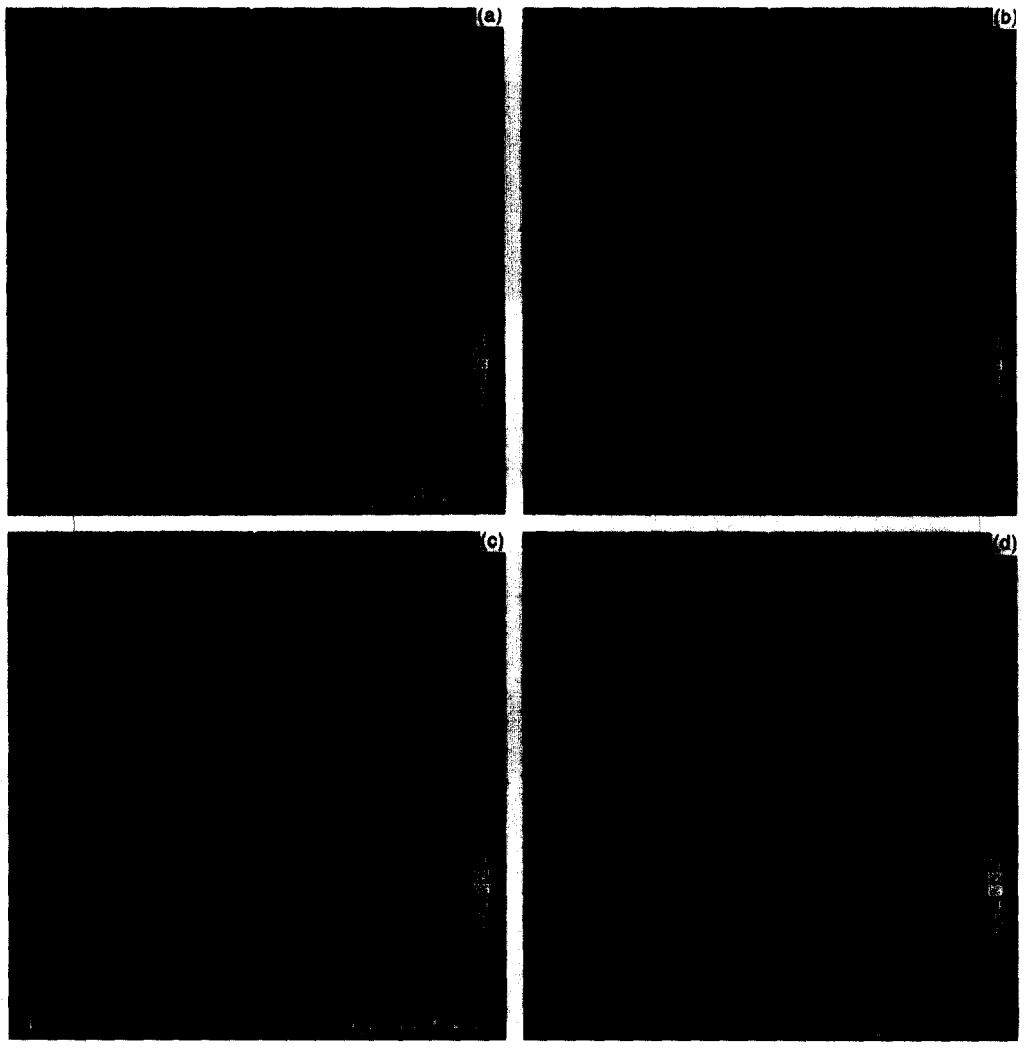

Plate 2. Five-day averaged OI SST maps for 2 March, 1 April, 1 May and 5 June 1993 for the mapping region shown in Fig. 1 along with a SST color table (°C). Also shown are the locations of four sets of grid points used for extraction of mean OI SST time series shown in Fig. 5 (crosses) and the cross-bank transect used for extraction of OI SST values shown in Fig. 13.

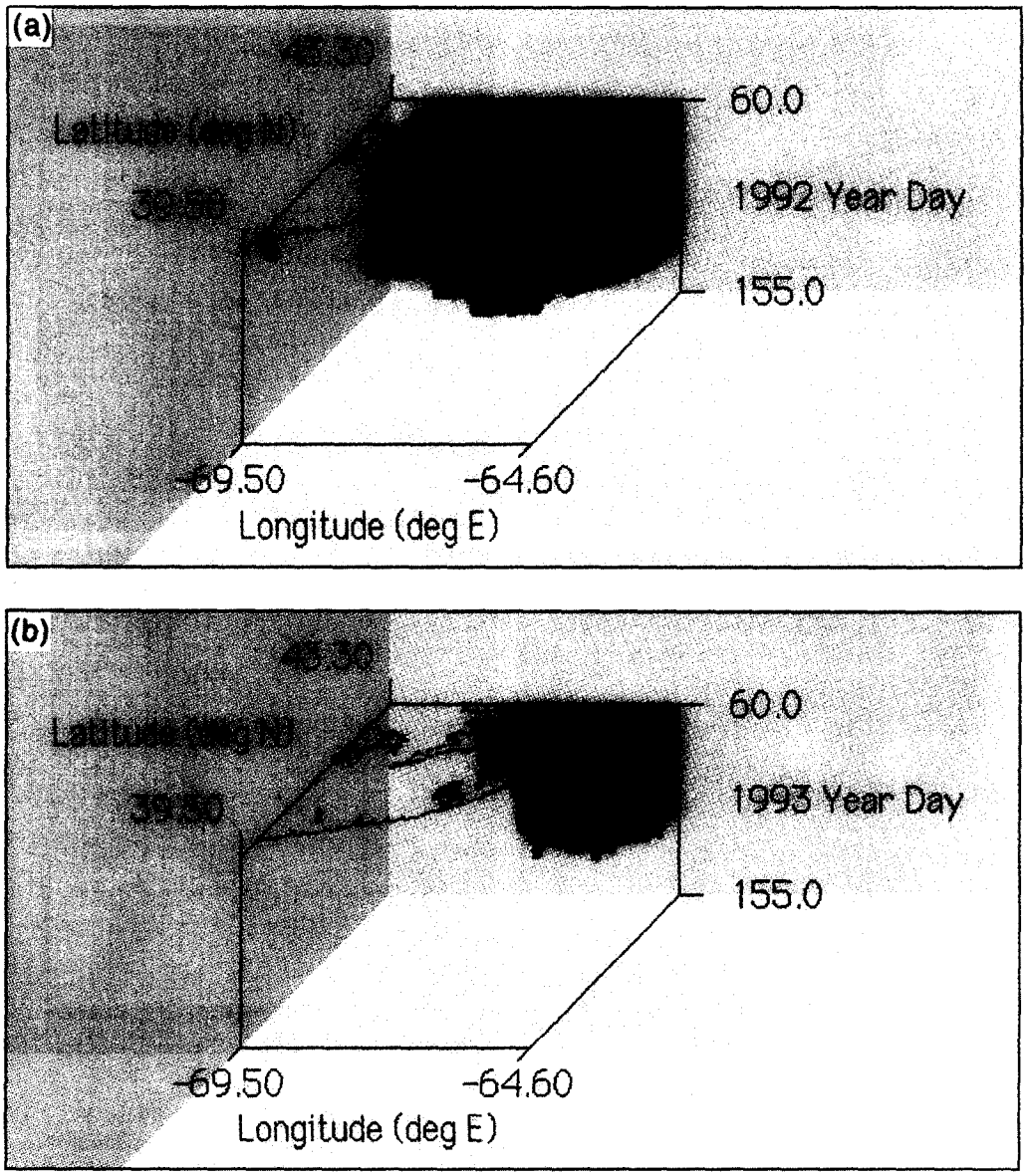

Plate 3. Volume rendering of SST ≤2.5°C from five-day averaged OI SST map time-series for 1992 (upper panel) and 1993 (lower panel) for the mapping region shown in Fig. 1.

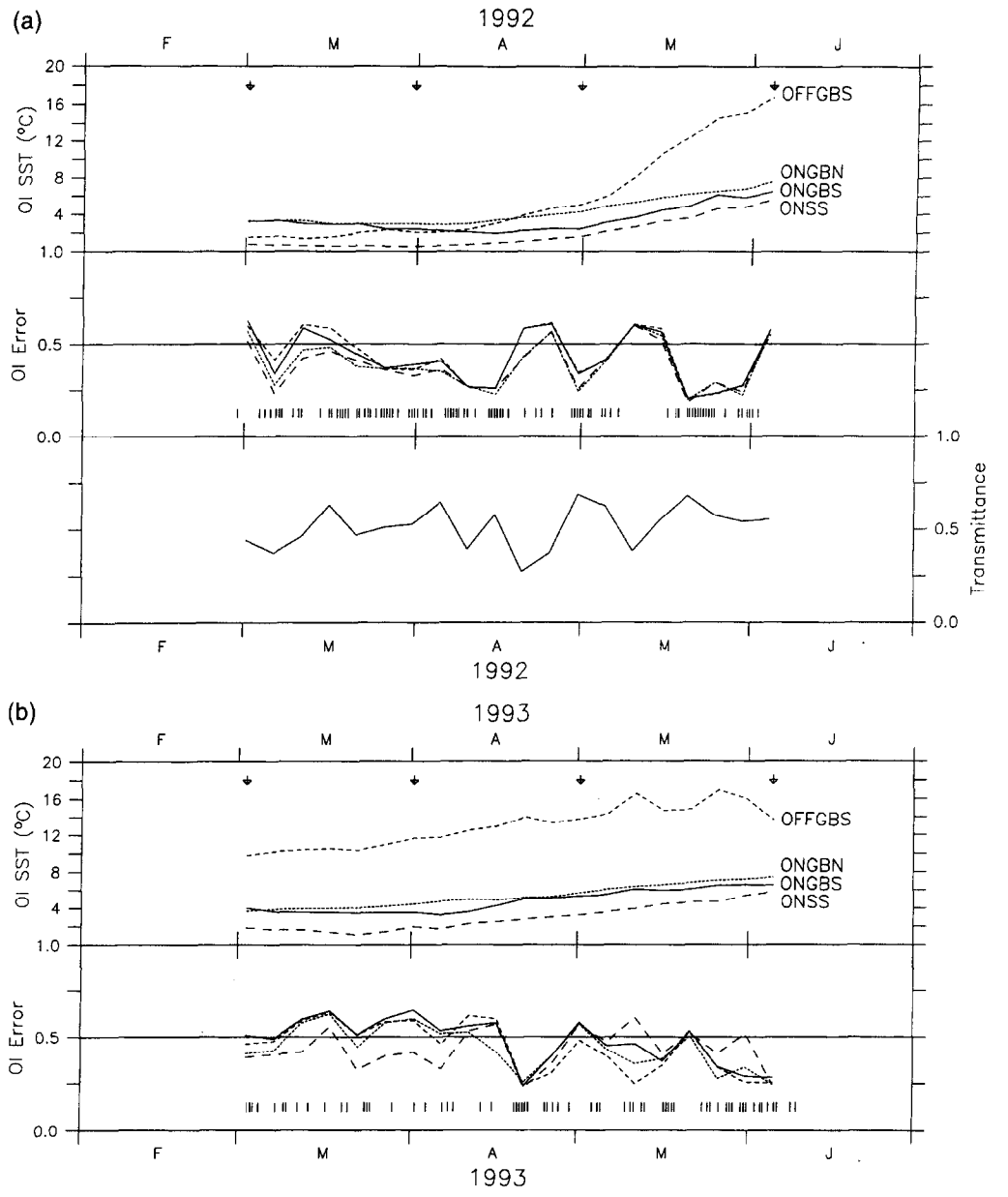

Fig. 5. Spring 1992 (a) and spring 1993 (b) five-day averaged OI SST and error time-series from ONGBS (solid line), OFFGBS (small dashes), ONSS (large dashes) and ONGBN (dotted line). Atmospheric transmittance at Woods Hole, Massachusetts is indicated for 1992 (a). Also shown are the dates of the OI SST maps given in Plates 1 and 2 (arrows) and dates of input AVHRR satellite images (vertical dashes).

Interannual variability of wind stress

Strong, southwestward-directed monthly-averaged wind stress occurred during October 1991, December 1992 and February 1993, relative to the 1967–1992 long-term mean, as a

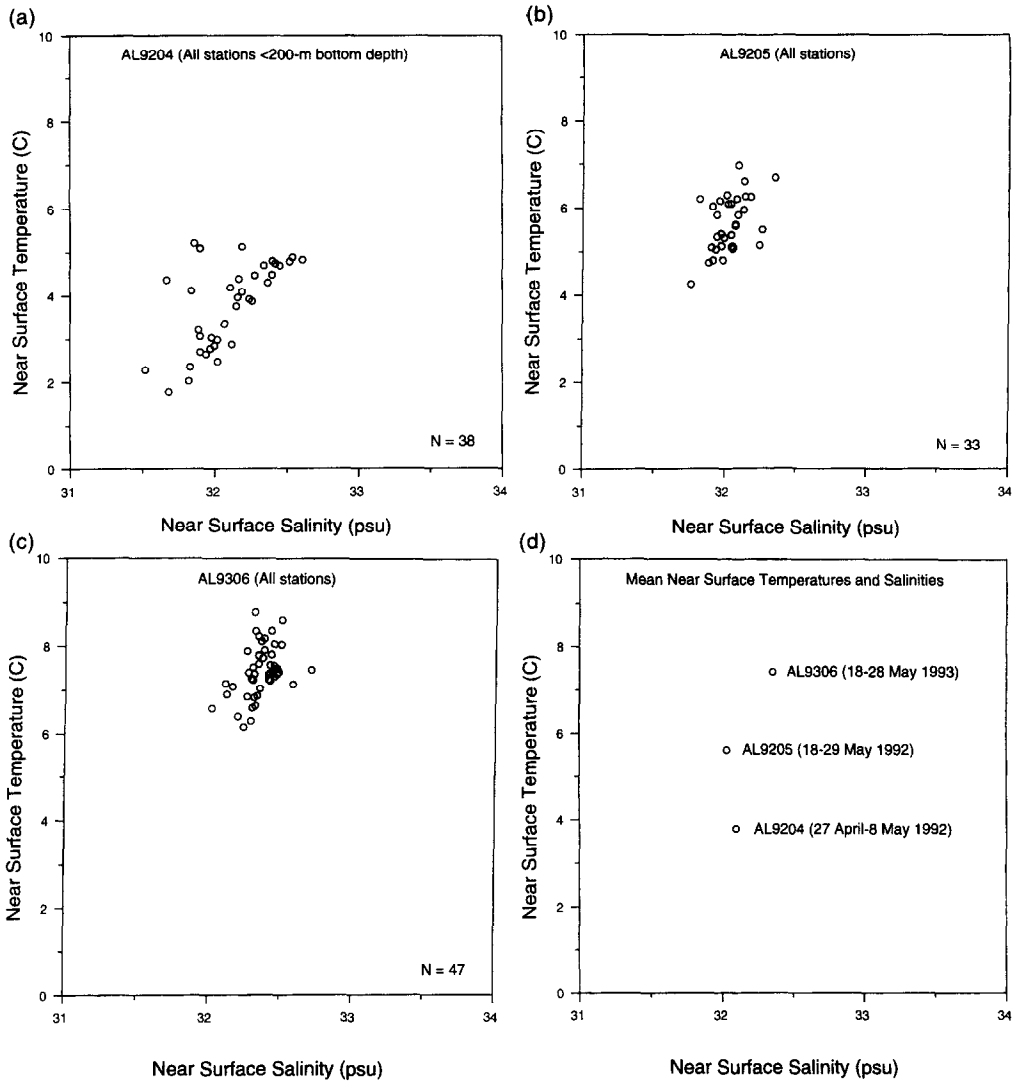

Fig. 6. Temperature–salinity correlation diagrams from near-surface measurements collected at all *Albatross IV* CTD stations (unless otherwise noted) shown in Figs 2 and 3. Also shown is the mean near-surface temperature and salinity correlation from each *Albatross IV* cruise (d).

result of long-lived cyclones (Fig. 9). Anomalous summer-like, northeastward-directed, stress occurred during January and March 1992 (Fig. 9). Other periods of high southwestward or northwestward stress occurred during May 1992 and again during March–April 1993.

Long-term mean monthly-averaged along-bank stress (τ^x) on Georges Bank changes sign in October and again in May during the transitional fall and spring seasons, respectively, but is greatest (positive) during summer when the prevailing northeastward-directed winds are nearly parallel to the isobaths along southern Georges Bank (Fig. 10). Long-term mean monthly-averaged cross-bank stress (τ^y) on Georges Bank is negative for every month of the

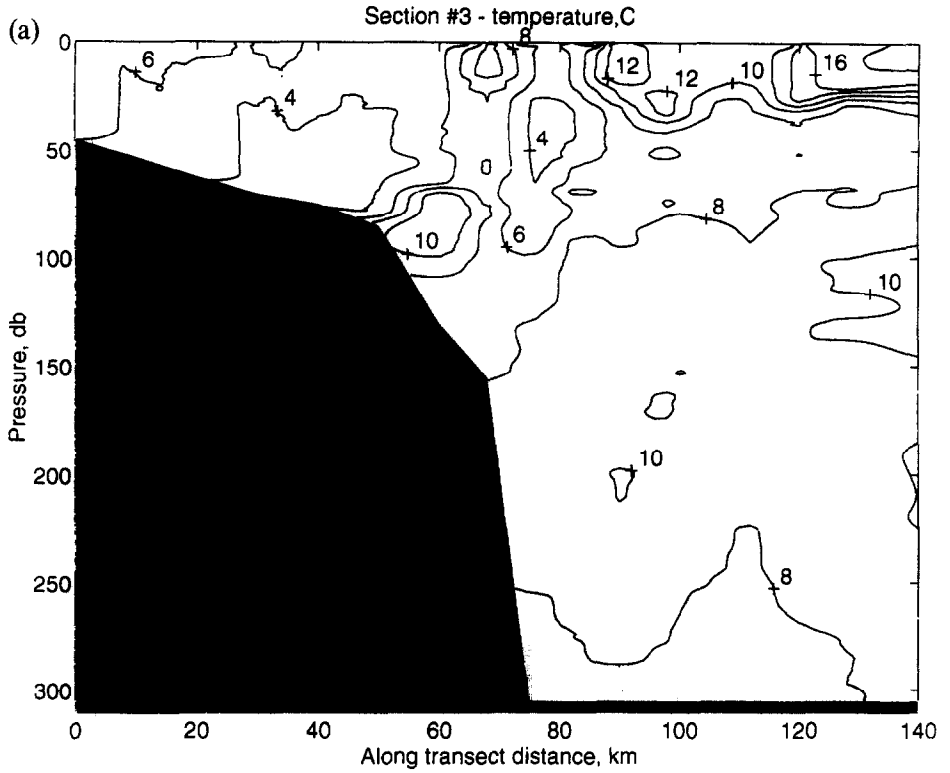

Fig. 7. (a) Temperature, (b) salinity and (c) density sections from R.V. *Endeavor* CTD transect shown in Fig. 2.

year but is greatest from November to April, reflecting strong wintertime southeastward-directed stresses (Fig. 10). Along-bank stress exhibited the largest fluctuations relative to the long-term mean from autumn to winter 1991–1992 and 1992–1993, with lesser fluctuations in the cross-bank stress occurring from autumn to spring (Fig. 10).

Interannual variability of St Lawrence river discharge

The maximum in the 38 year (1955–1992) long-term mean monthly-averaged St Lawrence River discharge (9.9×10^3 m^3 s^{-1}) occurs during April, with a minimum (8.0×10^3 m^3 s^{-1}) in January (Fig. 11). Monthly-averaged discharge from February to April 1991 was greater than 1 standard deviation higher than the long-term (1955–1992) mean, with a maximum of 11.4×10^3 m^3 s^{-1} during April, which decreased rapidly through the remainder of the year. Monthly-averaged discharge for spring 1992 was below normal, peaking at 9.5×10^3 m^3 s^{-1} during May.

Monthly cumulative volumes show divergence of the 1991 and 1992 values for January–April, with 1991 (1992) values greater than (less than) the long-term mean (Fig. 11). Differences between 1991 and 1992 cumulative volumes remained constant from May to June but later converged from July to December. However, percentage differences of cumulative volumes for the long-term mean and 1991 (relative to 1992) show that the St Lawrence River annually discharges ~9% more water by April of each year than it did by

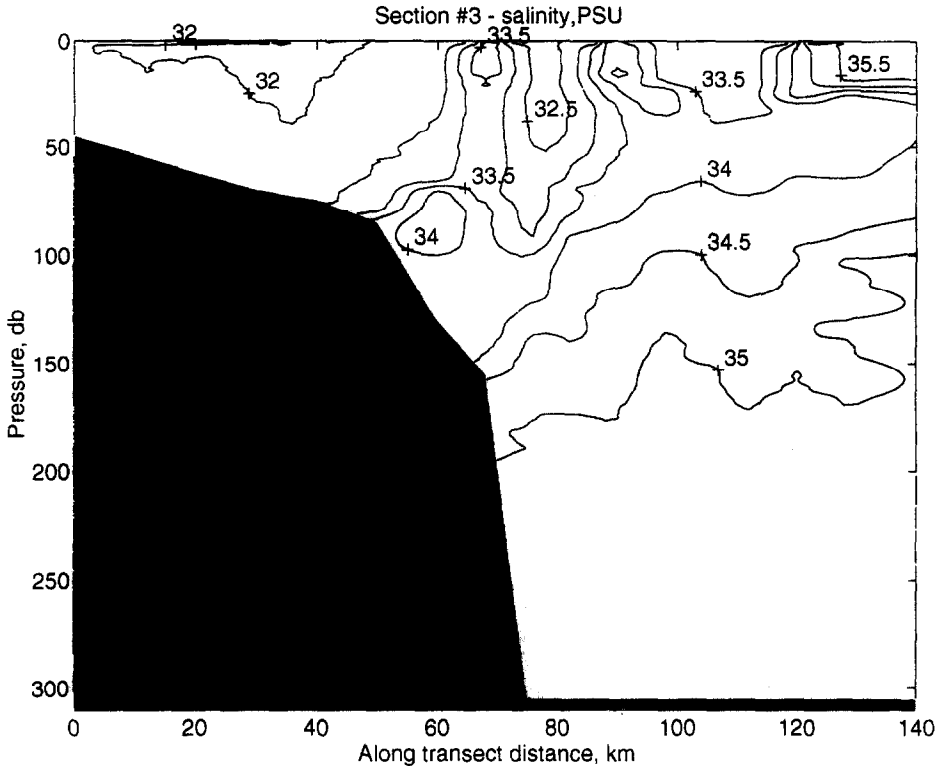

Fig. 7(b).

April 1992 and that it discharged ~25% more water by April 1991 than by April 1992, 1 year later (Fig. 11).

Spring 1992 *surface heat flux*

The largest contribution to Q_{net} during spring 1992 is from Q_{sw} (Fig. 12), similar to the annual cycle shown for monthly-averaged data in the Mid-Atlantic Bight (Bunker, 1976). Five-day averaged OI error time-series from 1992 reveal errors greater than 0.5× non-seasonal rms SST variability during data gaps when data were unavailable due to cloud-covered SST images (Fig. 5). Furthermore, the OI error time-series for 1992 display a strong correlation between all locations, showing that the temporal distribution of cloud-free observations at each site are related (Fig. 5). This result is similar to that deduced from correlations calculated between daily-averaged insolation data from eight coastal stations in the Gulf of Maine (Mountain *et al.*, 1996), which show a correlation of ~0.7 for distances equal to the maximum separation between our Georges Bank heat flux sites, supporting our assumption of identical Q_{sw} at each site. Furthermore, the inverse relationship between five-day averaged atmospheric transmittance estimated at Woods Hole and OI error time series at the three heat flux sites from April to June 1992 suggests that Woods Hole Q_{sw} values are valid at the offshore sites (Fig. 5).

Radiational losses due to Q_{lw} are substantial and always positive at all locations, while losses from Q_e are always positive and larger than Q_s losses (Fig. 12). Monthly-averaged Q_e

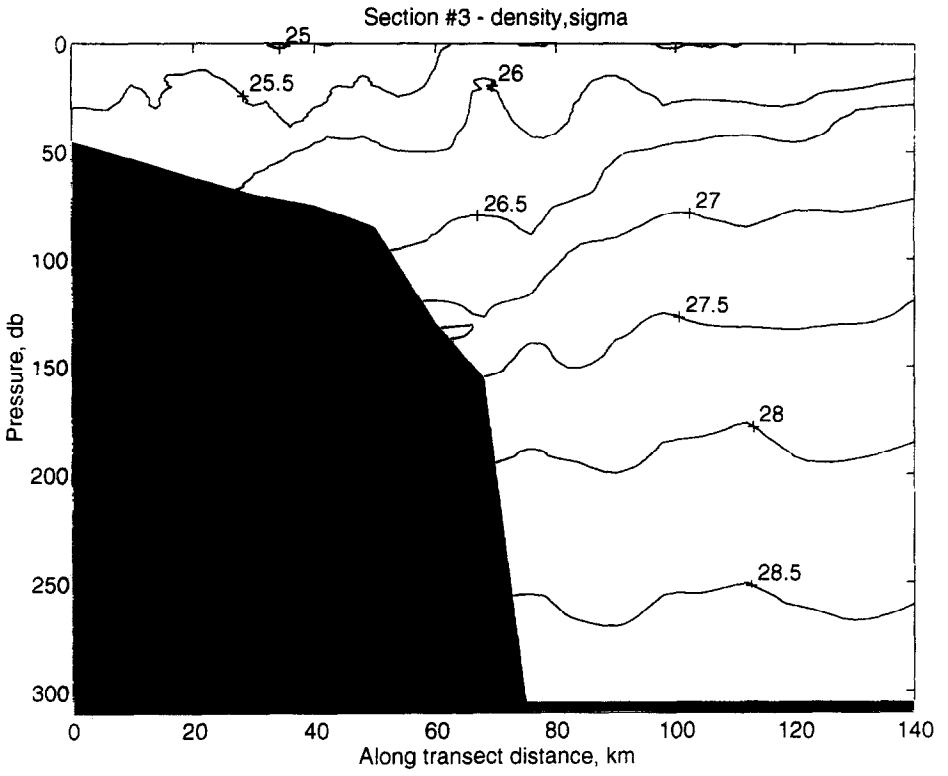

Fig. 7(c).

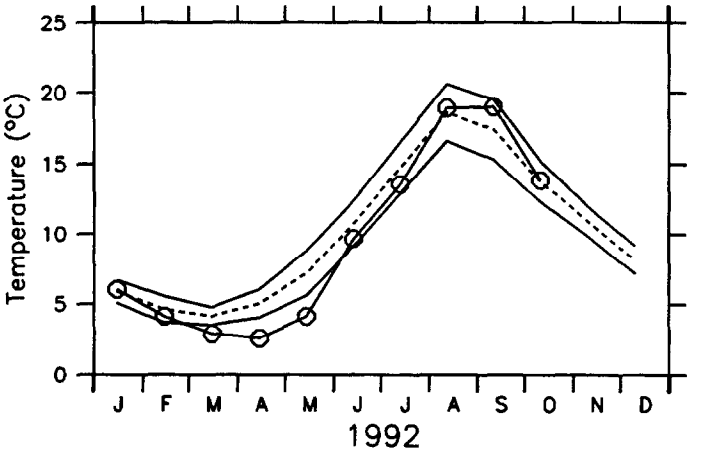

Fig. 8. Monthly-averaged near-surface temperature at NOAA data buoy 44011 for January–October 1992 (circles) and the 10-year (May 1984–March 1994) long-term mean (dashed) along with the ± 1 standard deviation values.

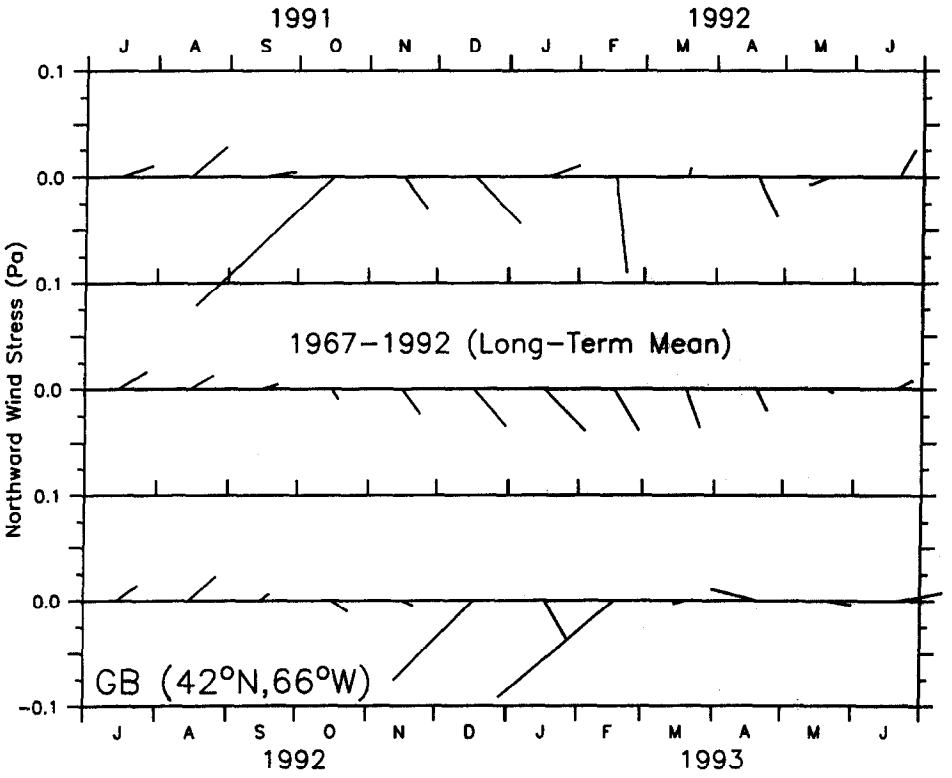

Fig. 9. Monthly-averaged wind stress on Georges Bank derived from FNOC model wind velocities computed at 42°N, 66°W (see Fig. 1) for July 1991–June 1992 (upper plot), 1967–1992 long-term mean (middle plot), and July 1992–June 1993 (lower plot).

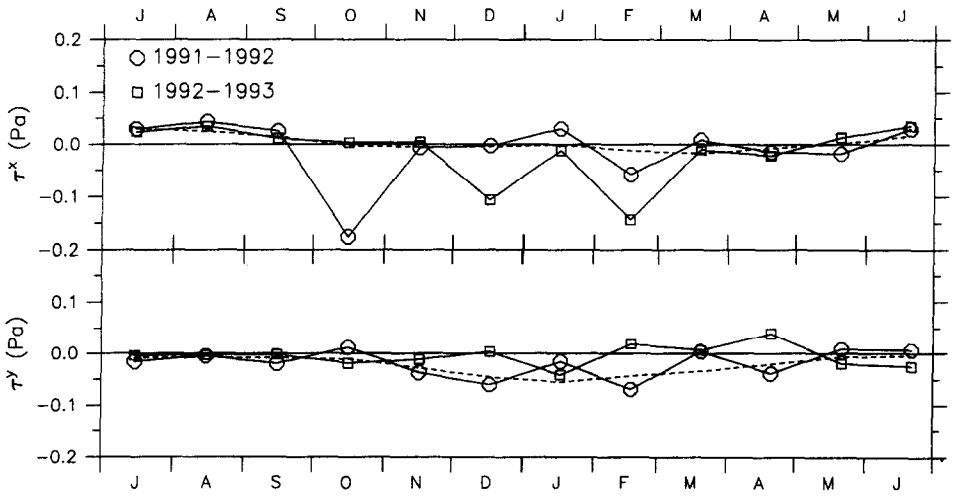

Fig. 10. Along-bank (τ^x) and cross-bank (τ^y) monthly-averaged wind stress on Georges Bank at 42°N, 66°W for July 1991–June 1992 (circles) and July 1992–June 1993 (squares). Long-term mean monthly-averaged stresses are also shown (dashed). $+\tau^x$ ($+\tau^y$) is oriented towards 43.2°T (313.2°T) (see Fig. 1).

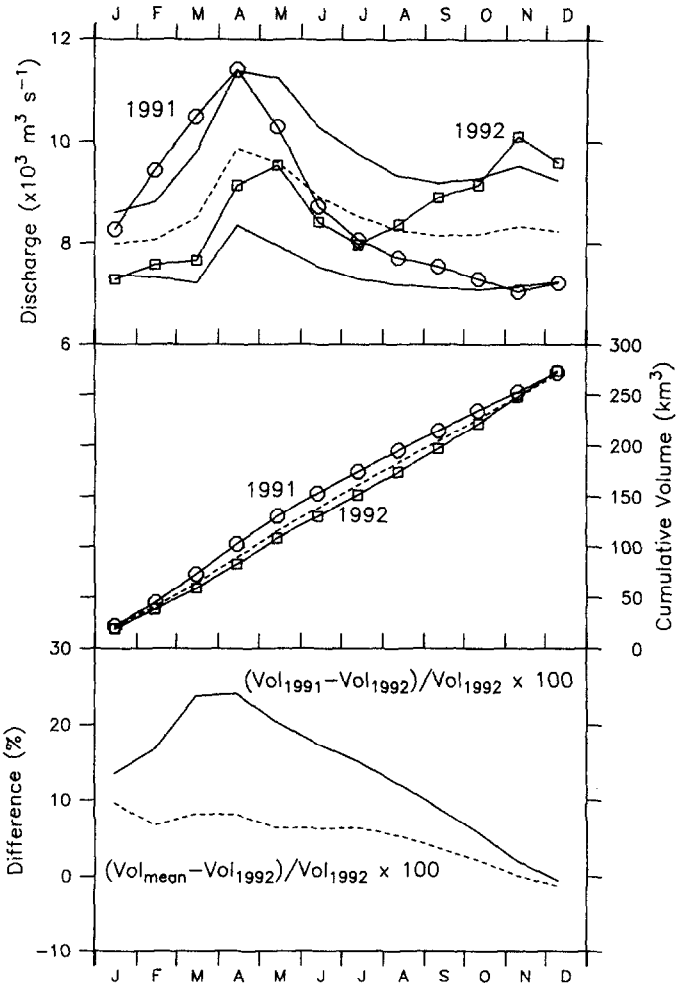

Fig. 11. Upper plot: monthly-averaged St Lawrence River discharge at gauging station 020A016 for 1991 (circles), 1992 (squares) and the 38 year (1955–1992) long-term mean (dashed) along with the ± 1 standard deviation values (solid). Middle plot: cumulative monthly-averaged discharge volume at gauging station 020A016 for 1991 (circles), 1992 (squares) and long-term (1955–1992) mean (dashed). Lower plot: per cent change between 1991 and 1992 cumulative monthly-averaged discharge volumes (solid line) and between the long-term mean and 1992 cumulative monthly-averaged discharge volumes (dashed line).

from the Mid-Atlantic Bight display a similar pattern for March–May, with a minimum Q_e loss occurring in May (Bunker, 1976). Rapidly increasing SST at OFFGBS during late April and May 1992 (Fig. 5) results in larger Q_e losses at OFFGBS during this period (Fig. 12).

Losses due to Q_s during spring 1992 were either negative though small (implying a heat gain) or close to zero at ONGBS and ONSS, except at the beginning of the record when Q_s was positive at all locations (Fig. 12). Thus, spring 1992 Q_s data at ONGBS and ONSS are similar to the annual cycle shown for monthly-averaged data in the Mid-Atlantic Bight (Bunker, 1976), which displayed a similar sign change from March to April as air

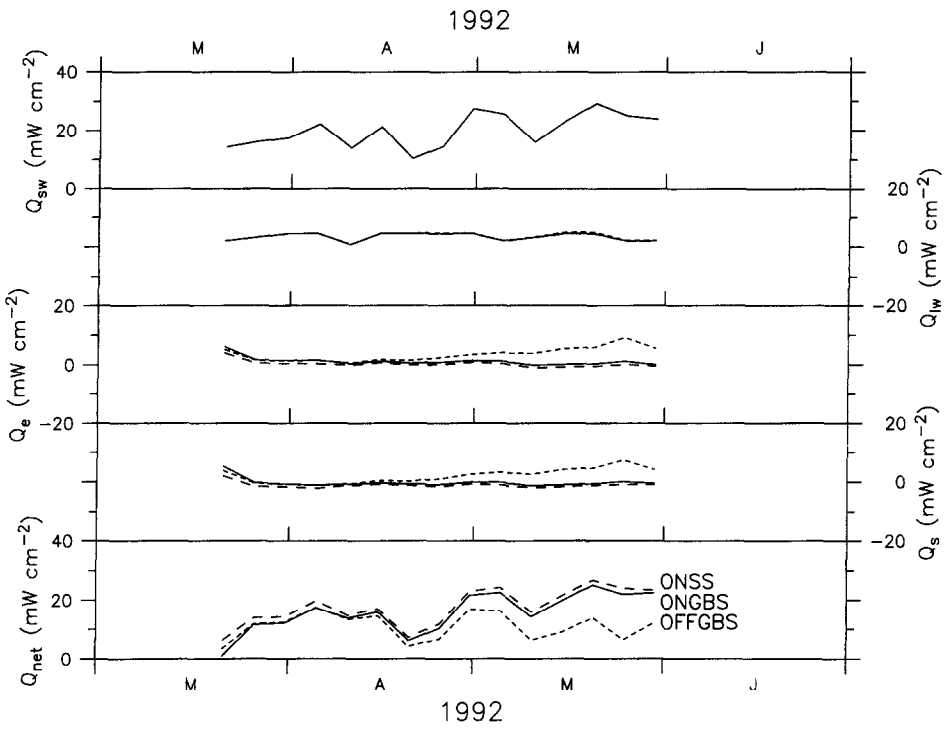

Fig. 12. Spring 1992 five-day averaged heat flux components at ONGBS (solid line), OFFGBS (small dashes), and ONSS (large dashes): Q_{sw} (net shortwave flux); Q_{lw} (net longwave flux); Q_e (latent heat flux); Q_s (sensible heat flux); Q_{net} ($Q_{net} = Q_{sw} - Q_{lw} - Q_e - Q_s$).

temperatures increased. Rapidly increasing SST at OFFGBS during late April–May 1992 (Fig. 5) results in larger Q_s losses at OFFGBS during this period (Fig. 12).

Five-day averaged Q_{net} is always positive and correlated at all locations during the period (Fig. 12). Differences between Q_{net} time-series are dominated by decreased Q_{net} at OFFGBS relative to ONGBS and ONSS, beginning in late April 1992 when larger sensible and latent losses began to occur, resulting in the smaller mean Q_{net} at OFFGBS for the period (Table 1).

DISCUSSION

The results from our analyses of historical data and hydrographic and satellite data from late winter–spring 1992 and 1993 from southern Georges Bank are compelling evidence that low salinity SSW is able to cross Northeast Channel onto Georges Bank during winter. Our results agree with earlier work (Hopkins and Garfield, 1981; EG&G, 1980; Flagg, 1987) and distributional patterns of *Calanus finmarchicus* on the Scotian Shelf and southern Georges Bank (Meise and O'Reilly, 1996). Furthermore, the differences between the near-surface water properties measured on southern Georges Bank during spring 1992 and 1993 reveal strong interannual variability in the transport and/or properties of SSW crossing Northeast Channel.

Table 2. Means and standard deviations of the five-day averaged advective heat flux (mW cm^{-2}) at three time series locations, spring 1992

Location	Q_{adv}
OFFGBS	-4.0 ± 9.9
ONGBS	-14.5 ± 9.6
ONSS	-10.6 ± 7.8

The effect of remote river discharge on southern Georges Bank

The extensive very cold, low salinity SSW plume that crossed Northeast Channel and lay southeast of Georges Bank by 1 January 1992, resulting in the exceptional spring 1992 occurrence of SSW on Georges Bank (Plate 1), did not occur during spring 1993 (Figs 2 and 3, Plates 1–3). Differences in near-surface salinity between spring 1992 and 1993 are consistent with the hypothesis that interannual variability of St Lawrence River discharge between April 1991 and 1992 (Fig. 11) affected the Bank's near-surface waters during winter 1992 and 1993, in agreement with the ~nine-month lag between the annual discharge maximum from RIVSUM and minimum salinity near Cape Sable (Smith, 1983, 1989b). However, comparisons between the 1966, 1971 and 1978 occurrences of less than 32.0 psu SSW on southern Georges Bank with St Lawrence River discharge data, for which discharge data are available for the year preceding each occurrence, show no relationship (Table 3). This result agrees with the lack of negative correlation between salinity anomalies near Cape Sable and lagged RIVSUM anomalies, apparently resulting from masking by local or other upstream effects (Smith, 1989b).

Mechanisms that may mask the effect of remote river discharge at Cape Sable include wind-driven upwelling of warm high salinity slope water in Northeast Channel, local discharge from Nova Scotia rivers, and melting ice from the Gulf of St Lawrence (Smith, 1989b). Warm-core Gulf Stream rings may cause masking by flooding Northeast Channel with high salinity water (Brooks, 1987) and through loss of low salinity shelf water by offshore advection along their eastern margins (Morgan and Bishop, 1977; Smith, 1978; Bisagni, 1983; Evans *et al.*, 1985; Garfield and Evans, 1987). Furthermore, variability in the number of warm-core Gulf Stream rings formed each year is high, from four during 1974 to 15 during 1988 (Sano and Wood, 1990), resulting in periods when rings are absent south of the Scotian Shelf (Celone and Chamberlin, 1980) relative to other years (Fitzgerald and Chamberlin, 1981).

The effect of wind stress on southern Georges Bank

Although several physical studies have addressed the response of shelf-break fronts to wind forcing for straight continental shelves (Csanady, 1978, 1984; Smith and Petrie, 1982; Ou, 1984; Ikeda, 1985; Chao, 1988), only one investigated the effect of wind forcing on a bank-trapped density front (Gawarkiewicz, 1993). Use of a non-linear primitive equation model showed that after a clockwise geostrophic flow is allowed to adjust for friction over an idealized bank, followed by application of a spatially uniform wind stress for three days, resulting surface velocities became asymmetrical and displayed a maximum (minimum) on the downwind (upwind) side of the bank to the left (right) of the wind direction

(Gawarkiewicz, 1993). Model velocities were shown to result from superimposition of the clockwise along-bank flow and a wind-driven surface Ekman layer (Gawarkiewicz, 1993), similar to the Ekman layer observed at the New England shelf-break front (Flagg, 1977). As a result of these flows, less-dense near-surface fluid is advected off the bank, weakening the near-surface horizontal density gradients (Gawarkiewicz, 1993). When the wind stress is suddenly removed, some fluid remains off the bank, resulting in a net loss of fluid from the region of the bank located downwind and to the right (Gawarkiewicz, 1993).

The mean circulation on Georges Bank is a clockwise gyre with maximum (minimum) speeds of 10–15 cm s^{-1} (3–10 cm s^{-1}) during summer (winter) (Butman *et al.*, 1987). Observed differences in the wind stress between late winter–spring 1992 and 1993 are considerable, showing significant periods of positive along-bank, summer-like, northeastward wind stress during January and March 1992 (Figs 9 and 10). If superposition of the Georges Bank mean circulation with a wind-driven surface Ekman layer follows the idealized model of Gawarkiewicz (1993), the observed offshore location of the shelf-slope front and SSW south of Georges Bank during late winter 1992 (Plate 1) may have resulted from a near-surface Ekman loss region (Lewis *et al.*, 1994), caused by northeastward wind stress during the period (Figs 9 and 10). Furthermore, increasing (decreasing) five-day averaged mean SST at OFFGBS (ONGBS) from mid-March to mid-April 1992 (Fig. 5) illustrates the on-bank movement of the shelf-slope front and the SST minimum associated with the 1992 SSW plume between 1 March and 30 April 1992 (Plate 1). Conversely, southwestward wind stress during February and March 1993 (Figs 9 and 10) could have caused a near-surface Ekman gain region (Lewis *et al.*, 1994) with the shelf-slope front remaining nearly coincident with the 200-m isobath, as observed along southern Georges Bank between 2 March and 1 May 1993 (Plate 2).

Five-day averaged along-bank wind stress from Georges Bank was compared with five-day averaged OI SST along the cross-bank transect shown in Plates 1 and 2 in order to investigate the relationship between along-bank wind stress and cross-bank movement of the shelf-slope front and the 1992 SSW plume. Data from 1992 show the SST minimum to correspond with the cold SSW plume moving on-bank from yearday 60 to 110, while the strong SST gradient associated with the shelf-slope front remained fixed at a distance of ~100-km southeast (off-bank) of the 200-m isobath along southern Georges Bank, despite fluctuations in the sign and magnitude of the along-bank wind stress (Fig. 13). However, the shelf-slope front then moved steadily bankward over a distance of ~100 km at an average speed of ~3 cm s^{-1} between yeardays 110 and 150 in good agreement with the calculated mean on-bank surface Ekman velocity of 3.9 cm s^{-1} computed from the mean along-bank (negative) windstress during the period. A similar comparison of five-day averaged along-bank wind stress and SST for the 1993 study period shows the shelf-slope front remaining nearly coincident with the 200-m isobath despite several fluctuations in the sign and magnitude of the along-bank wind stress (Fig. 13). Therefore, except for the on-bank movement of the shelf-slope front during late spring 1992, classical Ekman theory does not adequately explain the on-bank movement of the SSW plume during 1992 nor the immobile nature of the shelf-slope front during late winter 1992 and late winter–spring 1993. Clearly, cross-shelf motions in the vicinity of the shelf-slope front related to simple Ekman dynamics are complicated by low-frequency cross-shelf flow variability such as that related to currents associated with warm-core Gulf Stream rings or the effects of topographic Rossby waves radiated by warm-core rings (Smith and Petrie, 1982; Louis *et al.*, 1982). Furthermore, classical Ekman theory is not entirely applicable to low-frequency cross-shelf motions at the

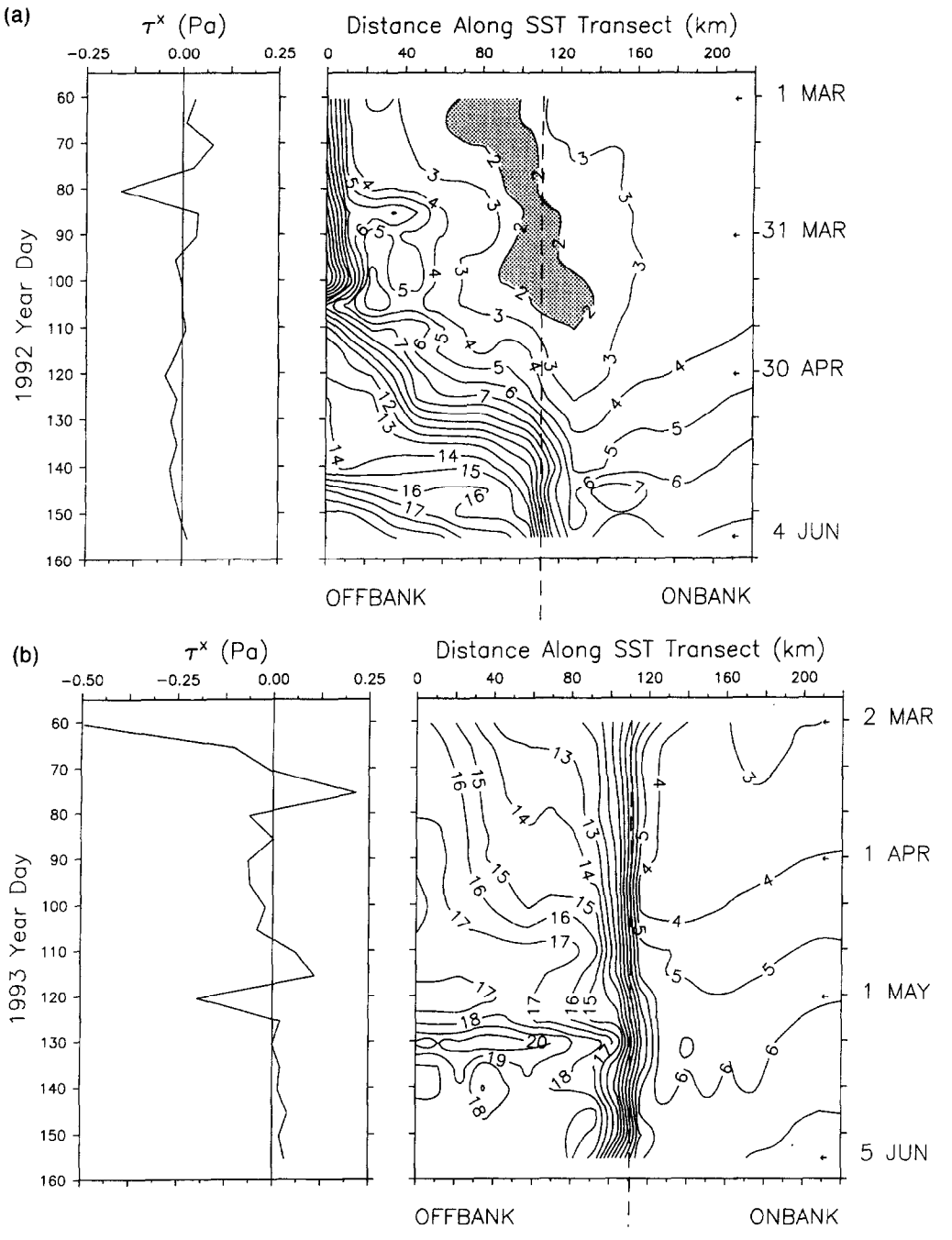

Fig. 13. Five-day averaged along-bank wind stress (τ^x) for Georges Bank and OI SST (°C) along the cross-bank transect shown in Plates 1 and 2 versus yearday for 1992 (upper panels) and 1993 (lower panels). $+\tau^x$ ($-\tau^x$) is directed towards 43.2°T (223.2°T). Also shown are the dates of the OI SST maps given in Plates 1 and 2 (small arrows). Vertical dashed line indicates the location of the 200-m isobath. SST ≤2°C is shaded.

shelf-slope front as shown by underprediction of offshore-directed currents and shelf water transport within a near-surface layer relative to observations on the Scotian Shelf (Smith and Petrie, 1982)

SSW heat flux and transport onto Georges Bank during spring 1992

The total time derivative of the heat energy per unit area contained within a surface mixed layer can be defined by

$$\frac{dE}{dt} = Q \tag{2}$$

where E is the heat energy per unit area and Q is the heat energy flux into the surface mixed layer. If we assume that the mixed layer is slab-like, i.e. no horizontal or vertical diffusion nor vertical velocity across the bottom of the mixed layer, expansion of equation (2) and rearrangement of terms yields

$$\frac{\partial E}{\partial t} = Q_{net} - \left(u\frac{\partial E}{\partial x} + v\frac{\partial E}{\partial y}\right) \tag{3}$$

where x and y (u and v) are the rotated along-bank and cross-bank coordinate directions (velocity components), respectively, and Q_{net} is the net surface heat flux defined by equation (1). Thus equation (3) shows that the local change in heat energy per unit area per unit time at any point is the difference between Q_{net} and the horizontal advective fluxes (Q_{adv}).

If we assume initially that Q_{adv} is zero and that Q_{net} is mixed rapidly throughout the mixed-layer, we can calculate time-series of predicted five-day averaged SST at ONGBS, OFFGBS and ONSS (Fig. 14) given mixed-layer depth, a starting (observed) SST and the five-day averaged Q_{net} at each location. Mixed-layer depth as a function of time was determined from the seasonal cycle of pycnocline depth, calculated from the 10-year NOAA/National Marine Fisheries Service's MARMAP data set at stations 153, 154 and 174, corresponding to ONGBS, OFFGBS and ONSS, respectively (Fig. 14).

Five-day averaged Q_{adv} time-series were calculated at each location as the difference between the observed and predicted SST time-series, integrated over the depth of the mixed-layer (Fig. 14). Errors for five-day averaged Q_{adv} are dominated by errors associated with Q_{net} and equal $\sim 3.5\ \mathrm{mW\ cm^{-2}}$. ONGBS shows the largest difference between observed and predicted SST, resulting in the largest mean advective heat flux: $-14.5\ \mathrm{mW\ cm^{-2}}$ (Fig. 14 and Table 2). Mean Q_{adv} for the period is significantly different from zero and negative at all locations, with Q_{adv} at ONGBS being almost four times larger than at OFFGBS (Table 3) and greater than three times larger than the annual mean value of $-4\ \mathrm{mW\ cm^{-2}}$ reported for Emerald Basin on the Scotian Shelf (Umoh and Thompson, 1994). Furthermore, mean Q_{adv} at ONSS is not significantly different from that at ONGBS, demonstrating that significant advection of cold water at ONSS from an upstream source is also required.

Standard deviations are the same magnitude (or larger) as mean Q_{adv} values, reflecting the large low-frequency ($\sim$20–30-day period) signals present in the data (Fig. 14). We speculate that the source of these fluctuations may be variations in vertical and horizontal mixing, neglected previously, caused by monthly and fortnightly (spring-neap) modulation of strong tidal currents present on Georges and Browns Bank. Addition of vertical and horizontal mixing terms to the right side of equation (3) would account for the apparent decrease in negative Q_{adv} at times of increased mixing of warmer near-bottom and offshore

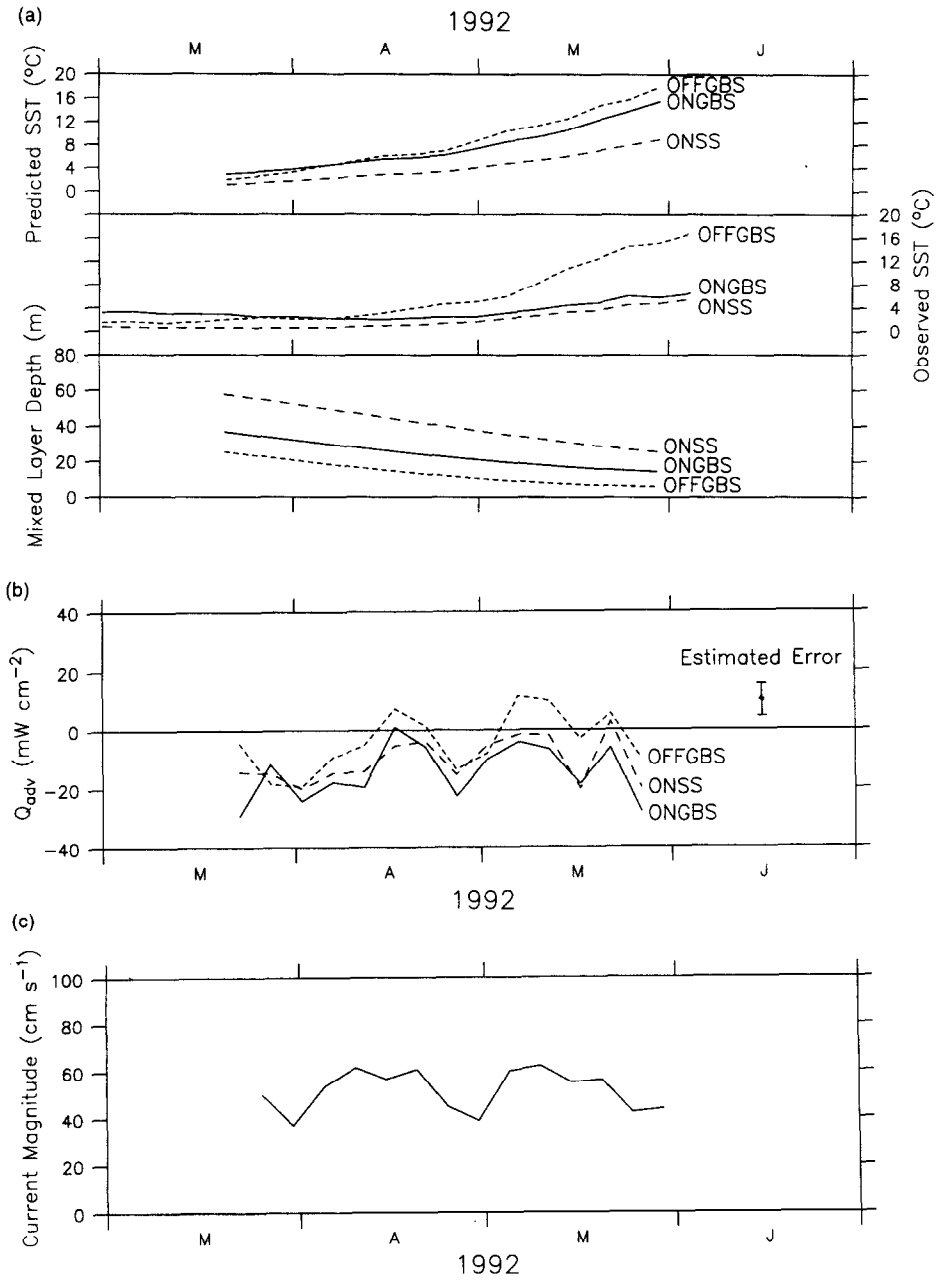

Fig. 14. Upper panel: predicted five-day averaged SST (upper plot), estimated five-day averaged OI SST (middle plot) shown in Fig. 5, and mixed-layer depth (lower plot). Middle panel: five-day averaged advective heat flux for spring 1992. ONGBS (solid line), OFFGBS (small dashes) and ONSS (large dashes). Lower panel: five-day averaged tidal current computed for a depth of 36 m using a harmonic method (Schureman, 1941) and M_2, N_2, S_2, O_1 and K_1 tidal constituents for 41°20'N, 67°15'W on Georges Bank (Moody *et al.*, 1984) and lagged by +3 days.

Table 3. Change (%) in cumulative (January–April) monthly-averaged discharge measured at St Lawrence River gauging station 020A016, 1 *year prior to occurrence of low salinity water (less than* 32.0 *psu) on Southern Georges Bank during May* 1966, 1971, 1978 *and* 1992, *relative to January–April* 1992

Year	% Change
1965	−20
1970	+3
1977	+8
1991	+25
1992	0

waters measured on southern Georges Bank near the 200-m isobath during late April–May 1992 (Manning *et al.*, 1995). This relationship is demonstrated by the correlation between phases of Q_{adv} and the spring-neap-modulated five-day averaged tidal current on Georges Bank (Fig. 14), after application of the 3-day lag between maximum tidal current and minimum SST described for southern Georges Bank (Bisagni and Sano, 1993). However, similar fluctuations in Q_{adv} also might be caused by a ~20-day-period along-shelf current variability within SSW flows located near the 200-m isobath caused by topographic Rossby waves radiated by warm-core Gulf Stream rings (Louis *et al.*, 1982).

In summary, mean and five-day averaged Q_{adv} suggest that significant advection of cold water onto southern Georges Bank and the southwestern Scotian Shelf is required, despite the large uncertainty in the various heat flux components and physical assumptions. If we assume that on-bank flow of SSW at ONGBS during 1992 was dominated by cross-channel flow from the Scotian Shelf at ONSS and may be characterized by a depth (width) of 40 m (40 km) as indicated from satellite and CTD data, the mean velocity and transport within the SSW plume can be calculated using the mean temperature gradient between ONGBS and ONSS, $-0.7 \pm 0.1 \times 10^{-7}$°C cm^{-1}. Calculations yield a mean velocity and transport of 13.4 cm s^{-1} and 0.21 Sv, with estimated errors of 4.0 cm s^{-1} and 0.06 Sv. Peak observed near-surface speeds, characteristic of the mean circulation on southern Georges Bank are 25 cm s^{-1} (15 cm s^{-1}) towards the southwest during summer (winter) (Naimie *et al.*, 1994). Estimated transports observed on southern Georges Bank are 0.65 Sv (0.43 Sv) during summer (winter) (Flagg *et al.*, 1982). Model Eulerian transports for bi-monthly flow fields calculated using tidal, density and wind forcing at a cross-bank section on southern Georges Bank are 0.42 Sv (0.53 Sv) during March–April (May–June) (Naimie *et al.*, 1994). Thus, mean velocity and transport estimates, calculated using our inverse method, are reasonable when compared with both observations and model output, suggesting that the flow of SSW onto Georges Bank during spring 1992 was robust throughout the period.

SUMMARY AND CONCLUSIONS

Analysis of historical data collected between 1912 and 1987 indicate the occasional occurrence of low salinity (less than 32.0 psu) water on southern Georges Bank during May, while none occurred during the month of April. Of the 10 years with adequate spatial coverage during the 76 year historical data period (1934, 1940, 1941, 1965, 1966, 1978, 1979, 1982, 1984 and 1985) water with salinity of less than 32.0 psu was found on southern

Georges Bank during May of 1941, 1966 and 1978, or three out of the 10 years. Composite monthly plots of near-surface salinity patterns derived from historical data and estimated rates of advection derived from near-surface drifters show that the southwestern Scotian Shelf is the immediate upstream source of the low salinity water occurring on southern Georges Bank during May.

Optimally-interpolated (OI) SST maps and hydrographic data from 1992 revealed cold (less than 2.0°C), low salinity (less than 32.0 psu) Scotian Shelf Water (SSW) extending from the southwestern Scotian Shelf to a position offshore of the 200-m isobath along southern Georges Bank on 1 March 1992. The shelf-slope front, separating the cold SSW from warm slope water, was located far ($\sim$100 km) seaward of the 200-m isobath during early March 1992. On-bank movement of the SSW during April 1992 resulted in monthly-averaged near-surface temperatures on the Bank's southern flank, decreasing to an April minimum of $\sim$2.5°C, and being greater than 1 standard deviation lower (up to $\sim$3.0°C colder) than the long-term mean temperature at NOAA buoy 44011 by May 1992. When compared with 1992, the significantly higher temperatures and salinities of near-surface waters on southern Georges Bank during late winter–spring 1993 show large interannual variability in the transport and/or properties of SSW crossing Northeast Channel onto Georges Bank.

The hypothesis that enhanced St Lawrence River discharge may cause the occurrence of low salinity water on southern Georges Bank during late spring was examined. While lower (higher) salinities measured during spring 1992 (1993) are consistent with higher (lower) St Lawrence River discharge during spring 1991 (1992) and the $\sim$nine-month lag between the annual RIVSUM discharge maximum and minimum salinity near Cape Sable, similar comparisons between the occurrence of low salinity (less than 32.0 psu) SSW on southern Georges Bank during May 1966, 1971 and 1978 and lagged St Lawrence River discharge show no similar relationship. This suggests that the occurrence of low salinity water on southern Georges Bank is not directly related to variations in the upstream river discharge. This result is consistent with the observed lack of negative correlation between salinity anomalies near Cape Sable and lagged RIVSUM anomalies.

Although an idealized model of wind forcing on a bank-trapped density front shows that near-surface flow is related to superposition of an Ekman layer and the along-bank gyral circulation, evidence from late winter–spring 1992 and 1993 shows that except for the on-bank movement of the shelf-slope front during late spring 1992, simple Ekman theory does not explain on-bank movement of the SSW plume during 1992 nor the immobile nature of the shelf-slope front during late winter 1992 and late winter–spring 1993. Simple Ekman dynamics may be complicated by low-frequency cross-shelf flow variability arising from various effects related to the presence of warm-core Gulf Stream rings.

Surface heat flux and satellite-derived SST estimates from Georges Bank and the Scotian Shelf together with a slab mixed-layer model allowed estimation of the advective heat flux and transport of SSW flowing onto Georges Bank from the Scotian Shelf during late winter–spring 1992. Results showed:

1. Mean advective heat flux onto southern Georges Bank (the southwestern Scotian Shelf) during March–May 1992 is $-14.5\,\mathrm{mW\,cm^{-2}}$ ($-10.6\,\mathrm{mW\,cm^{-2}}$) with an estimated error of $\sim 3.5\,\mathrm{mW\,cm^{-2}}$, demonstrating that advection of cold water is required at both locations.
2. Significant low-frequency ($\sim$20–30-day period) fluctuations in advective heat flux occurring at all locations during the period may have been caused by variations in mixing

related to the spring-neap modulation of tidal currents present on Georges and Browns Bank.

3. Mean velocity and transport of SSW onto Georges Bank during March–May 1992 were estimated to be 13.4 cm s^{-1} and 0.21 Sv, assuming a SSW depth (width) of 40 m (40 km). Despite errors of 4.0 cm s^{-1} and 0.06 Sv, the velocity and transport estimates are reasonable when compared with current observations and transport estimates on southern Georges Bank, demonstrating that flow of SSW onto Georges Bank was robust during late winter–spring 1992.

At this time, the dynamical mechanism controlling the flow of SSW across Northeast Channel is unknown. Preliminary results with an idealized numerical circulation model indicate that a purely barotropic steady current cannot break the potential vorticity barrier imposed by the steep bottom topography around Northeast Channel (Williams, 1995). These results imply that the dominant mechanism(s) are likely to be baroclinic and possibly time dependent.

Acknowledgements—The authors would like to thank P. Cornillon, University of Rhode Island Graduate School of Oceanography, for providing AVHRR satellite data and image analysis software. The authors would also like to thank D. Husby, NOAA/National Marine Fisheries Service, for providing FNOC model winds, R. Payne, Woods Hole Oceanographic Institution, for providing solar radiation data and R. Bibeau, Environment Canada, for providing river discharge data. Special thanks to D. Mountain and J. Manning, NOAA/National Marine Fisheries Service, and C. Davis and S. Gallager, Woods Hole Oceanographic Institution for providing hydrographic data, and to G. Strout, NOAA/National Marine Fisheries Service, for assisting with the heat flux calculations. Optimal interpolation software was developed and provided by D. Chelton, Oregon State University. Image analysis software was developed by R. Evans, O. Brown and A. Li, University of Miami, under Office of Naval Research funding. The continuing support of the Miami group is gratefully acknowledged. The authors would also like to thank two anonymous reviewers for providing helpful comments to improve the manuscript. This work was completed under support provided by the NOAA Office of Global Programs as part of the joint NSF/NOAA U.S.-GLOBEC Georges Bank Northwest Atlantic Program. This is contribution number 45 of the U.S. GLOBEC program, funded jointly by the NSF and NOAA.

REFERENCES

Bakun A. (1975) Daily and weekly upwelling indices, west coast of North America, 1967–1973. *NOAA Technical Report* NMFS SSRF–693, NOAA/NMFS, Seattle, WA, 114 pp.

Bigelow H. B. (1927) Physical oceanography of the Gulf of Maine. *Bulletin of the United States Bureau of Fisheries*, **40**, 511–1027.

Bisagni J. J. (1983) Lagrangian current measurements within the eastern margin of a warm-core Gulf Stream ring. *Journal of Physical Oceanography*, **13**, 709–715.

Bisagni J. J. (1992) Differences in the annual stratification cycle over short spatial scales on southern Georges Bank. *Continental Shelf Research*, **12**, 415–435.

Bisagni J. J. and M. H. Sano (1993) Satellite observations of short timescale sea surface temperature variability on southern Georges Bank. *Continental Shelf Research*, **13**, 1045–1064.

Bisagni J. J., D. J. Gifford and C. M. Ruhsam (1996) The spatial and temporal distribution of the Maine Coastal Current during 1982. *Continental Shelf Research*, **16**, 1–24.

Brooks D. A. (1987) The influence of warm-core rings on slope water entering the Gulf of Maine. *Journal of Geophysical Research*, **92**, 8183–8196.

Brown W. S. and R. C. Beardsley (1978) Winter circulation in the western Gulf of Maine: Part 1. Cooling and water mass formation. *Journal of Physical Oceanography*, **8**, 265–277.

Brownlee K. A. (1965) *Statistical theory and methodology in science and engineering*. J. Wiley and Sons, New York, 590 pp.

Budyko M. I. (1974) *Climate and life*. Academic Press, New York.

Bunker A. F. (1976) Computations of surface energy flux and annual air–sea interaction cycles of the North

Atlantic Ocean. *Monthly Weather Review*, **104**, 1122–1140.

Butman B., J. W. Loder and R. C. Beardsley (1987) The Seasonal Mean Circulation: observation and theory. In: *Georges Bank*, R. H. Backus, editor, MIT Press, Cambridge, MA, pp. 125–138.

Cayula J.-F. and P. Cornillon (1992) Edge detection algorithm for SST images. *Journal of Atmospheric and Oceanic Technology*, **9**, 67–80.

Celone P. J. and J. L. Chamberlin (1980) Anticyclonic warm-core Gulf Stream eddies off the northeastern United States in 1978. *Annales Biologiques*, **35**, 50–55.

Chao S.-Y. (1988) Wind-driven motion of estuarine plumes. *Journal of Physical Oceanography*, **18**, 1144–1166.

Chapman D. C., J. A. Barth, R. C. Beardsley and R. G. Fairbanks (1986) On the continuity of mean flow between the Scotian Shelf and the Middle Atlantic Bight. *Journal of Physical Oceanography*, **16**, 758–772.

Chapman D. C. and R. C. Beardsley (1989) On the origin of shelf water in the Middle Atlantic Bight. *Journal of Physical Oceanography*, **19**, 384–391.

Chelton D. B. and M. G. Schlax (1991) Estimation of time averages from irregularly spaced observations: With application to Coastal Zone Color Scanner estimates of chlorophyll concentration. *Journal of Geophysical Research*, **96**, 14,669–14,692.

Chen C. (1992) Variability of currents in Great South Channel and over Georges Bank: Observation and modelling. Ph.D. Thesis, MIT/WHOI Joint Program in Oceanography, Massachusetts Institute of Technology, Cambridge, MA.

Colton J. B., R. R. Marak, S. Nickerson and R. F. Stoddard (1968) Physical, chemical and biological observations on the continental shelf, Nova Scotia to Long Island, 1964–1966. United States Fisheries and Wildlife Service Data Report 23, 190 pp.

Cornillon P., C. Gilman, L. Stramma, O. Brown, R. Evans and J. Brown (1987) Processing and analysis of large volumes of satellite-derived thermal infrared data. *Journal of Geophysical Research*, **92**, 12,993–13,002.

Csanady G. T. (1978) Wind effects on surface to bottom fronts. *Journal of Geophysical Research*, **83**, 4633–4640.

Csanady G. T. (1984) The influence of wind stress and river runoff on a shelf–sea front. *Journal of Physical Oceanography*, **14**, 1383–1392.

Davis C. S., S. M. Gallager, M. S. Berman, L. R. Haury and J. R. Strickler (1992) The video plankton recorder (VPR): Design and initial results. *Archive Fur Hydrobiologie Beiheft*, **36**, 67–81.

DeYoung B. and C. L. Tang (1989) An analysis of Fleet Numerical Oceanographic Center winds on the Grand Banks. *Atmosphere–Ocean*, **27**, 414–427.

EG&G (1980) Thirteenth quarterly report. Appendix F. Analysis report. Prepared for the New York OCS Office, Bureau of Land Management, by EG&G Environmental Consultants, Waltham, MA, 194 pp.

Evans R. H., K. S. Baker, O. B. Brown and R. C. Smith (1985) Chronology of warm-core ring 82B. *Journal of Geophysical Research*, **90**, 8803–8811.

Fairbanks R. G. (1982) The origin of continental shelf and slope water in the New York Bight and Gulf of Maine: Evidence from $H_2{}^{18}O/H_2{}^{16}O$ ratio measurements. *Journal of Geophysical Research*, **87**, 5796–5808.

Fitzgerald J. L. and J. L. Chamberlin (1981) Anticyclonic warm-core Gulf Stream eddies off the northeastern United States in 1979. *Annales Biologiques*, **36**, 44–51.

Flagg C. N. (1977) The kinematics and dynamics of the New England continental shelf and shelf/slope front. Ph.D. Thesis, MIT/WHOI Joint Program in Oceanography, Massachusetts Institute of Technology, Cambridge, MA.

Flagg C. N. (1987) Hydrographic structure and variability. In: *Georges Bank*, R. H. Backus, editor, MIT Press, Cambridge, MA, pp. 108–124.

Flagg C. N., B. A. Magnell, D. Frye, J. J. Cura, S. E. McDowell and R. I. Scarlet (1982) Interpretation of the physical oceanography of Georges Bank. Final report prepared for the New York OCS office, Bureau of Land Management, by EG&G Environmental Consultants, Waltham, MA, 901 pp.

Fofonoff N. P. and H. Bryden (1975) Specific gravity and density of seawater at atmospheric pressure. *Journal of Marine Research*, **33**, 69–82.

Friehe C. A. and K. F. Schmitt (1976) Parameterization of air–sea interface fluxes of sensible heat and moisture by the bulk aerodynamic formulas. *Journal of Physical Oceanography*, **6**, 801–809.

Garfield N. and D. L. Evans (1987) Shelf water entrainment by Gulf Stream warm-core rings. *Journal of Geophysical Research*, **92**, 13,003–13,012.

Gawarkiewicz G. (1993) Steady wind forcing of a density front over a circular bank. *Journal of Marine Research*, **51**, 109–134.

Hopkins T. S. and N. Garfield (1979) Gulf of Maine intermediate water. *Journal of Marine Research*, **37**, 103–139.

Hopkins T. S. and N. Garfield (1981) Physical origins of Georges Bank water. *Journal of Marine Research*, **39**, 465–500.

Ikeda M. (1985) Wind effects on a front over the continental shelf slope. *Journal of Geophysical Research*, **90**, 9108–9118.

Joyce T. M. (1987) Meteorology and air–sea interaction. In: *The marine environment of the U.S. Atlantic Continental Slope and Rise*, J. D. Milliman and W. R. Wright, editors, Jones and Bartlett, Boston, MA, pp. 5–26.

Koslow J. A., R. H. Loucks, K. R. Thompson and R. W. Trites (1986) Relationships of St Lawrence River outflow with sea surface temperature and salinity in the Northwest Atlantic. In: *The role of freshwater outflow in coastal marine ecosystems*, S. Skreslet, editor, Springer-Verlag, Berlin.

Large W. G. and S. Pond (1981) Open ocean momentum flux measurements in moderate to strong winds. *Journal of Physical Oceanography*, **11**, 324–336.

Lewis C. V. W., C. S. Davis and G. Gawarkiewicz (1994) Wind forced biological–physical interactions on an isolated offshore bank. *Deep-Sea Research II*, **41**, 51–73.

Limeburner R. and R. C. Beardsley (1982) Seasonal hydrography and circulation over Nantucket Shoals. *Journal of Marine Research*, **40** suppl., 371–406.

Limeburner R. and R. C. Beardsley (1989) Lagrangian circulation in the Great South Channel and on Georges Bank during summer. In: *Proceedings of third Georges Bank research workshop*. Bedford Institute of Oceanography (Abstract only).

Louis J. P., B. D. Petrie and P. C. Smith (1982) Observations of topographic Rossby waves on the continental margin off Nova Scotia. *Journal of Physical Oceanography*, **12**, 47–55.

Manning J., T. Holzwarth-Davis, M. Taylor, T. Rotunno, D. Mountain and G. Lough (1995) Georges Bank Stratification Study: 1992 Data Report. NEFSC Ref. Doc. 95–10, NOAA/NMFS, Woods Hole, MA, 109 pp.

Meise C. and J. E. O'Reilly (1996). Spatial and seasonal patterns in abundance and age-composition of *Calanus finmarchicus* in the Gulf of Maine and on Georges Bank: 1977–1987. *Deep-Sea Research II*, **43**, 1473–1501.

Moody J. A., B. Butman, R. C. Beardsley, W. Boicourt, W. S. Brown, P. Daifuku, J. D. Irish, D. A. Mayer, H. O. Mofjeld, B. Petrie, S. Ramp, P. Smith and W. R. Wright (1984) Atlas of tidal elevation and current observations on the Northeast American continental shelf and slope. *U.S. Geological Survey Bulletin*, **1611**, 122.

Morgan C. W. and J. M. Bishop (1977) An example of Gulf Stream eddy-induced water exchange in the mid-Atlantic bight. *Journal of Physical Oceanography*, **7**, 472–479.

Mountain D. G. (1991) The volume of Shelf Water in the Middle Atlantic Bight: seasonal and interannual variability, 1977–1987. *Continental Shelf Research*, **11**, 251–267.

Mountain D. G., G. A. Strout and R. C. Beardsley (1996). Surface heat flux in the Gulf of Maine. *Deep-Sea Research II*, **43**, 1533–1546.

Naimie C. E., J. W. Loder and D. R. Lynch (1994) Seasonal variation of the three-dimensional residual circulation on Georges Bank. *Journal of Geophysical Research*, **99**, 15,967–15,989.

NODC (1991) Global ocean temperature and salinity profiles: Vol. 1—Atlantic, Indian, and Polar Oceans. CD-ROM NODC-02, US Dept. of Commerce, NOAA/NESDIS/NODC, 1825 Connecticut Avenue, NW, Washington, DC 20235.

Ou H. W. (1984) Wind-driven motion near a shelf-slope front. *Journal of Physical Oceanography*, **14**, 985–993.

Payne R. E. (1972) Albedo of the sea surface. *Journal of the Atmospheric Sciences*, **29**, 959–970.

Redfield A. C. (1939) The history of a population of *Limacina retroversa* during its drift across the Gulf of Maine. *Biological Bulletin*, **76**, 26–47.

Reed R. K. (1976) An estimation of net long-wave radiation from the oceans. *Journal of Geophysical Research*, **81**, 5793–5794.

Reed R. K. (1977) On estimating insolation over the ocean. *Journal of Physical Oceanography*, **7**, 482–485.

Sano M. H. and G. B. Wood (1990) Anticyclonic warm-core Gulf Stream rings off the Northeastern United States in 1989. Northwest Atlantic Fisheries Organization, SCR Doc. 90/25, Serial Number N1742, 16 pp.

Simpson J. J. and C. A. Paulson (1979) Mid-ocean observations of atmospheric radiation. *Quarterly Journal of the Royal Meteorological Society*, **105**, 487–502.

Schureman P. (1941) *Manual of harmonic analysis and prediction of tides*. U.S. Department of Commerce, Coast and Geodetic Survey, Special Publication no. 98, 317 pp.

Smith P. C. (1978) Low-frequency fluxes of momentum, heat, salt and nutrients at the edge of the Scotian shelf. *Journal of Geophysical Research*, **83**, 4079–4096.

Smith P. C. (1983) The mean seasonal circulation off southwest Nova Scotia. *Journal of Physical Oceanography*, **13**, 1034–1054.

Smith P. C. (1989a) Circulation and dispersion on Browns Bank. *Canadian Journal of Fisheries and Aquatic Sciences*, **46**, 539–559.

Smith P. C. (1989b) Seasonal and interannual variability of current, temperature and salinity off southwest Nova Scotia. *Canadian Journal of Fisheries and Aquatic Sciences*, **46**, 4–20.

Smith P. C. and B. D. Petrie (1982) Low-frequency circulation at the edge of the Scotian Shelf. *Journal of Physical Oceanography*, **12**, 28–46.

Sutcliffe W. H., R. H. Loucks and K. F. Drinkwater (1976) Coastal circulation and physical oceanography of the Scotian shelf and the Gulf of Maine. *Journal of the Fisheries Research Board of Canada*, **33**, 98–115.

Thomson R. E. (1983) A comparison between computed and measured oceanic winds near the British Columbia coast. *Journal of Geophysical Research*, **88**, 2675–2683.

Umoh J. J. and K. R. Thompson (1994) Surface heat flux, horizontal advection, and the seasonal evolution of water temperature on the Scotian Shelf. *Journal of Geophysical Research*, **99**, 20,403–20,416.

Williams W. J. (1995) The adjustment of barotropic currents at the shelf break to a sharp bend in the shelf topography. M.S. Thesis, MIT/WHOI Joint Program in Oceanography, Massachusetts Institute of Technology, Cambridge, MA.